European Journal of Agronomy 150 (2023) 126945

Contents lists available at ScienceDirect

European Journal of Agronomy

journal homepage: www.elsevier.com/locate/eja

Climate warming may accelerate apple phenology but lead to divergent dynamics in late-spring frost and poor pollination risks in main apple production regions of China

Xiaoya Ru [a,b], Jie Zhou [a,b], Kaiyuan Gong [a,b], Zhihao He [a,b], Zhanwu Dai [c], Meirong Li [d,e], Xinxin Feng [f], Qiang Yu [e,g], Hao Feng [g], Jianqiang He [a,b,e,*]

[a] Key Laboratory for Agricultural Soil and Water Engineering in Arid Area of Ministry of Education, Northwest A&F University, Yangling 712100, Shaanxi, China
[b] Institute of Water-Saving Agriculture in Arid Areas of China, Northwest A&F University, Yangling 712100, Shaanxi, China
[c] Beijing Key Laboratory of Grape Science and Enology and Key Laboratory of Plant Resources, Institute of Botany, the Chinese Academy of Sciences, Beijing 100093, China
[d] Shaanxi Meteorological Service Center of Agricultural Remote Sensing and Economic Crops, Xi'an 710014, Shaanxi, China
[e] Key Laboratory of Eco-Environment and Meteorology for the Qinling Mountains and Loess Plateau, Shaanxi Provincial Meteorological Bureau, Xi'an 710015, Shaanxi, China
[f] Nanjing Shuxi Intelligent Technology Co., Ltd., Nanjing, Jiangsu 210019, China
[g] State Key Laboratory of Soil Erosion and Dryland Farming on the Loess Plateau, Institute of Water and Soil Conservation, Northwest A&F University, Yangling 712100, Shaanxi, China

ARTICLE INFO

Keywords:
Apple phenology
First flowering
Late-spring frost
Poor pollination
Model ensemble
Climate change

ABSTRACT

Frost exposure and poor pollination are great challenges for the cultivation of perennial orchard systems such as apples, whose adaptive capacity to climate impacts is limited. Unfortunately, such climatic risks remained largely unexplored due to the complexity in future climate predictions, uncertainties in apple phenological simulations, and difficulties in quantifications of risks of late-spring frost and poor pollination. Here, focusing on the main apple production Sub-regions I–IV (i.e., the Loess Plateau, the Bohai Bay, the Southwest Cool Highland, and Xinjiang) in China, we used an ensemble of seven phenological models to estimate changes in apple first flowering and fruit-setting. Based on phenological sensitivity window proposed, we evaluated the late-spring frost risk and climatic risk of poor pollination based on two individual indices developed for these two kinds of meteorological risks. The phenology model ensemble was driven by climatic data derived from an ensemble of 27 global climate models (GCMs) from CMIP6 to simulate apple phenology in two periods of 2021 – 2060 (Near Future) and 2061 – 2100 (Far Future) under two climate scenarios of SSP245 and SSP585. Model ensemble could largely improve phenology prediction accuracy. Our results also confirmed the general earlier occurrence of apple phenological stages and the shortening of phenological sensitive windows. The first flowering advanced about 0.19 – 0.32 $d \bullet y^{-1}$ and fruit-setting advanced about 0.24 – 0.47 $d \bullet y^{-1}$. Although the shortening of phenological sensitivity window might decrease frost frequency in some regions and reduce the general risk of late-spring frost (e.g. in Sub-region II), the increase of frost intensity could offset this kind of alleviation and even exacerbate frost risks in Sub-regions I and IV. Finally, except for Sub-region III and a few sites in Sub-regions I and IV, shifts in climatic risks of poor pollination in spatial contrasts were lower than late-spring frost risk. This highlighted late-spring frosts would be more possibly the reason for apple yield or quality losses than the unfavorable climatic pollination conditions under climate change. Model ensemble provides a realistic assessment for quantifying future risks of late spring frost and poor pollination in apple production systems, and helps to identify urgent meteorological risks and provide options for apple production systems in response to climate change.

* Corresponding author at: Key Laboratory for Agricultural Soil and Water Engineering in Arid Area of Ministry of Education, Northwest A&F University, Yangling 712100, Shaanxi, China.
E-mail address: jianqiang_he@nwsuaf.edu.cn (J. He).

https://doi.org/10.1016/j.eja.2023.126945
Received 5 April 2023; Received in revised form 28 July 2023; Accepted 7 August 2023
Available online 17 August 2023

1. Introduction

Ongoing and predicted climate change has already modified the phenology (i.e., the occurrence of development stages) of many temperate fruit trees in various regions (Rodríguez et al., 2021). Among the globally cultivated and consumed fruits, apple holds a prominent position (Liang et al., 2022). In 2020, approximately 43 million metric tons of apples were produced from a total area of 1.98 million hectares in China (FAO, 2021, https://www.fao.org/faostat/en/). Some studies recorded the phenological changes in apple growth period under climate change, among which the advancing of apple phenology was predominant in last several decades (Fernandez et al., 2022; Kalvāne et al., 2021; Kunz and Blanke, 2022; Legave et al., 2013). For example, through analyzing historic records of phenological events (budburst and blossom) of apples from 1977 to 2004 at six different locations in Japan, Fujisawa and Kobayashi (2010) reported an advance rate of apple phenophases up to $0.21 - 0.35$ d•y^{-1} due to the rising air temperature. In contrast, Legave et al. (2013) observed late dormancy release and consequently delayed first flowering timing of apple in the Mediterranean region. The phenological response of apples to climate change can vary greatly across different regions (Menzel et al., 2006), increasing the possibility of some agronomic risks.

Frost risk and climate-related poor pollination risk, which mainly happened in spring sensitive phenological stage, can lead to low levels of set fruit and subsequently negatively influence apple yield (Drepper et al., 2022; Kaukoranta et al., 2010). Global warming, which raises temperatures, seems to make frosts less likely. However, the advance of phenophase could increase the exposure of apple flowers to frost risk according to some previous reports (Masaki, 2019; Pfleiderer et al., 2019), since earlier phenology increased the likelihood for late-spring frost to coincide with apple sensitive phenological stage. In addition to frost injury, changes in phenology caused by climate change might also exacerbate the risk of poor pollination during apple flowering stage through changing the external environment that pollinators and pollinating organs depend on (Wilcock and Neiland, 2002; Wyver et al., 2023). In most cases, the occurrence of the frost and poor pollination coincided with flowering and fruit-setting stages, resulting in simultaneous negative effects on apple production. Unfortunately, the current understanding and quantification of these dual climate risks remained largely unexplored due to the complexity in future climate predictions, uncertainties in apple phenological simulations, and difficulty in quantifications of risks of frost and poor pollination.

Different hypotheses about the biochemical mechanism of dormancy breaking in fruit trees have derived various models for the phenological prediction of fruit trees (Hufkens et al., 2018; Legave et al., 2015; Pertille et al., 2022). For apple trees, it was assumed that dormancy could be classified into endo- and eco-dormancy, representing two different sub-phases of internal clock of apple trees (Pfleiderer et al., 2019). The need for cold temperatures has been proposed as the characteristic of endodormancy phase (first phase, represented as chilling requirements), while warm temperature conditions are thought to be the main driver of leaf, inflorescence, and fruit primordium development during ecological dormancy (second phase, described as heat forcing) (Legave et al., 2015). Given these relatively solid physiological assumptions (i.e., considering either forcing alone or both chilling and forcing), different types of phenological models (including one-phase or two-phase models) were widely used to project the responses of tree phenological stages to climate change (Eccel et al., 2009; Fernandez et al., 2022; Pertille et al., 2022). However, most of published studies were commonly based on only one model, which was often chosen rather arbitrarily (Legave et al., 2008). This could lead to huge uncertainties in model projection results sometimes. To minimize the uncertainties and errors of model projections, the ensemble approach has been greatly advocated recently (Gritti et al., 2013; Rosenzweig et al., 2013; Ruane et al., 2017). Predictions from a group of models (i.e., an ensemble of multiple models) often provide more robust information for decision support than one model (Yan et al., 2021). Moreover, an efficient ensemble of models should integrate a variety of different phenological models (Migliavacca et al., 2012), which could help reveal the tradeoff effects between chilling and forcing on regulating the occurrence of phenological events in apple trees. In addition, most studies on phenology of fruit trees were based on climatic data derived from single climate model downscaled regionally (Cho et al., 2020; Fraga and Santos, 2021). Few attentions were paid to the reduction of prediction uncertainties when coupling climate models with the phenological models. It is urgently necessary to use an ensemble of multiple phenological models and multiple global climate models (GCMs) to reduce the prediction uncertainties arising from model structures (Melaas et al., 2016; Tao et al., 2018).

Climate change may increase the time overlap between flowering and frost events (Drepper et al., 2022), but also change the pollination environments during flowering on the other hand (Polce et al., 2014). Concerns about frost risk were usually associated with the advancing in phenology stage of fruit trees, while changes of pollination environments were accompanied by the advanced or delayed phenology stages (Drepper et al., 2022; Iovane et al., 2021). Different flowering stages are differently affected to frost, while full flowering is recognized as the most sensitive phenophase (Kunz and Blanke, 2022). Thus, frost risk occurrence was often measured through comparing the advancing of flowering dates and the last frost dates (Farajzadeh et al., 2010; Masaki, 2019; Pfleiderer et al., 2019). However, this method may underestimate actual frost risk since the apple phenophase, spanning from the first flowering stages to early fruit setting, is highly susceptible to frost damage. Unfortunately, studies offering definitive quantification of the duration of the first flowering and fruit-setting stages of apples are exceedingly scarce. As a result, the accurate quantification of frost impact remains elusive. Correspondingly, another concerned risk of poor pollination, which can also occur during the interval between apple first flowering and fruit-setting, is not be tackled directly either. This was the main reason why the exploration of pollination risk at apple flowering stage was rare by far. Indeed, the pollinating activities of pollinators (e.g., bees) can be negatively affected by low temperature and rainfall (Iovane et al., 2021). Moreover, excessively warm temperatures can limit the growth rate of pollen tubes and cause pollination deficits (Lorite et al., 2020; Yoder et al., 2009). Given the great concerns about frost risk and poor pollination risks in apple production, the relevant concepts and research methods need to be updated nowadays accordingly.

To optimize the estimation of apple first flowering and fruit-setting dates and provide an improved evaluation of potential frost and poor pollination risks under future climate warming, an ensemble of several different phenological models coupled with global climate models were used to estimate the duration of critical apple phenophase from first flowering to fruit-setting, which was defined as the phenological sensitivity window in this study. Furthermore, we used two indices of AFD (accumulated frost days) and AFDD (accumulated frost degree-days) to quantify the risk of late-spring frosts in apple phenological sensitivity window. The other two indices of CR (Cold and rainy events) and WT (Warm temperatures events) were used to quantify the risk of climatic risk of poor pollination.

The main objective of this study was to assess the dynamics of apple phenology and investigate the changes of late-spring frost risk and climatic risk of poor pollination under future climate warming in main apple producing regions of China. To achieve this goal, (1) an ensemble of seven different phenological models were calibrated and validated to simulate apple first flowering and fruit-setting dates based on phenological observations obtained from the representative sites in four apple-producing sub-regions of China; (2) the phenological sensitivity window from apple first flowering to fruit-setting was calculated for each representative site under two climate warming scenarios of SSP245 and SSP585; and (3) the frequency and intensity of frost risk and poor pollination risk were analyzed within apple phenological sensitivity

window for each representative site.

2. Materials and methods

2.1. Study area

China is the largest apple producer in the world. The apple production reached about 43 million tons in 2020, accounting for approximately 50% of the world's total (FAO, 2021, https://www.fao.org/faostat/en/). Fig. 1 provided an illustration of the primary cultivation areas for apple trees in China, which can be categorized into four distinct sub-regions. These sub-regions are identified as follows: the Loess Plateau (Sub-region I), encompassing provinces such as Shaanxi, Gansu, Shanxi, Henan, and Ningxia; the Bohai Bay (Sub-region II), including provinces like Shandong, Liaoning, and Hebei; the Southwest Cool Highland (Sub-region III), covering provinces such as Yunnan, Sichuan, and Guizhou; and Xinjiang (Sub-region IV). These four sub-regions are the most suitable regions for apple cultivation in China. The *'Fuji'* cultivar covers about 65% of the apple trees in these sub-regions (FAO, 2021, https://www.fao.org/faostat/en/). The Loess Plateau is the largest apple production base in China, where the planting area and production account for about 57.2% and 53.0% of whole country, respectively (Tang et al., 2021). The Bohai Bay is the second-largest apple cultivation area, where the planting area and production account for about 26.9% and 36.0% (Tang et al., 2021). The total planting area and production of the Southwest Cool Highland and Xinjiang cover about 15.9% and 11.0%, respectively. In addition to the experimental sites in ten apple orchards (purple triangle in Fig. 1), we randomly selected 53, 34, 7, and 6 representative apple-growing sites for future analysis in Sub-regions I, II, III, and IV, respectively (black solid dots in Fig. 1). A detailed description of the experimental sites in Sub-regions I–IV was available in Table S1.

2.2. Data sources

2.2.1. Apple phenology observation data

The records of two phenological stages of *'Fuji'* apple cultivar were collected, namely "first flowering" (representing the date of the first flower opening, referred to as BBCH 60) and "fruit-setting" (signifying the date when the young fruit begins to grow after the petals fall, referred to as BBCH 70) (Chapman and Catlin, 1976; Meier et al., 1994). The apple phenology observation datasets were obtained from the Shaanxi Meteorological Bureau (http://sn.cma.gov.cn/) and the Nanjing Shuxi Intelligent Technology Co., Ltd. (http://www.shuxitech.com/). The series of first flowering dates ranged from 1972 to 2020, with a total of 107 observations available. The series of fruit-setting dates ranged from 2016 to 2020, with a total of 80 observations available (Table S1).

2.2.2. Climate data

Daily weather data were obtained from the on-site weather stations for eight apple phenology observation sites in the sub-regions (Fig. 1). Since the rest two experimental sites had no weather station, we used county-level daily weather data obtained from the China Meteorological Data Network (https://data.cma.cn/) instead. Likewise, we obtained daily weather data in 1980 – 2020 (Baseline period) from the China Meteorological Data Network for the representative apple-growing sites in the sub-regions. Future climatic data were obtained from 27 Global Climate Models (GCMs; Table S2) for two future periods of 2021 – 2060 (Near Future) and 2061 – 2100 (Far Future) at each of the representative apple-growing sites. The 27 GCMs were downloaded from the Coupled Model Intercomparison Project Phase 6 (CMIP6; https://esgf-node.llnl.gov/projects/cmip6/) of the Intergovernmental Panel on Climate Change in the Sixth Assessment Report (CMIP6-IPCC-AR6). The IPCC-AR6 advocated five new climate change scenarios based on the Shared Socioeconomic Pathways (SSPs), namely SSP119, SSP126,

Fig. 1. Map of the four main apple producing sub-regions (Sub-region I: the Loess Plateau, II: the Bohai Bay, III: the Southwest Cool Highland, and IV: Xinjiang) in China. The purple triangles represent the ten apple orchards for phenological observations in this study. The black solid dots are the representative apple-growing sites in different sub-regions.

SSP245, SSP370, and SSP585 (IPCC, 2021). In this study, we only focused on the intermediate (SSP245) and high (SSP585) warming scenarios. Since the future climate data are monthly grid datasets with a spatial resolution of 1°, a statistical downscaling approach developed by the NSW Department of Primary Industries, Wagga Wagga Agricultural Institute was used to convert the original data to site-specific daily weather data in this study. More information about this downscaling approach can be found in Liu and Zuo (2012).

2.3. Apple phenology simulation models

Seven different phenological models were used to simulate the first flowering and fruit-setting stages of '*Fuji*' apple trees, including one simple linear regression model and six process-based phenological models (Table 1). The linear regression model (Equation 1) does not consider the specific biological processes, only using phenophase as the dependent variable and daily average temperature (from 1st January to 31st March) as the independent variable to describe the correlations between phenophase and driving factors (Asse et al., 2020). The other six models described the causality relationships between apple phenophase and the exterior environments (mainly temperature and day length) (Asse et al., 2020; Chuine et al., 1999).

These six process-based apple phenology models can be divided into two types: one-phase models and two-phase models. The one-phase models (including the Thermal Time model, Uniforc model, and M1 model; Equations 2–4) are based on the assumption that a phenological event will occur once sufficient heat forcing is accumulated (Chuine et al., 1999). The one-phase models do not take endodormancy into account. Accordingly, apple first flowering and fruit-setting stages are triggered when specified total forcing requirements (F*) are met after a fixed date (t1) with a rate of forcing (R_f). Thus, the specified total chilling requirements (C*) of apple trees are assumed to have been met before the fixed starting date (Eccel et al., 2009; Legave et al., 2008). Usually, daily mean temperature is first transformed via the specified forcing equation in each model (Table 1) and subsequently accumulated as the forcing unit. For the Thermal Time model, forcing units are the total degrees above the critical temperature (T_c) and t1 is set to January, 1st (DOY=1; DOY = day of year). The M1 model uses the same settings but adds a correction for the required forcing based on the day length (Blümel and Chmielewski, 2012). The Uniforc model is like the Thermal Time model but has the forcing units transformed via a sigmoid function.

The two-phase models (including the Alternating, Unichill model, and Sequential model; Equations 5–7) consider both the specified total

Table 1
Brief introduction of the seven phenological models used to simulate apple first flowering and fruit-setting dates in this study. 31 DOY (Day of year) refers to Jan. 31 and − 67 DOY refers to Oct. 26 of last year. Negative DOY number refers to the DOY in prior season.

Model name	Description	Equation	Reference
Linear	Simple linear regression model	$DOY = \beta_1 + \beta_2 T_{mean}$ (1)	(Boyer, 1973)
Thermal Time	Classic growing degree day model (One-phase) using a fixed temperature threshold above which forcing accumulates.	$\sum_{t=t_1}^{DOY} R_f(T_i) \geq F^*$ (2) $R_f(T_i) = \max(T_i - T_c, 0)$	(Cannell and Smith, 1983)
Uniforc	One-phase forcing model using a sigmoid function for forcing accumulates.	$\sum_{t=t_1}^{DOY} R_f(T_i) \geq F^*$ (3) $R_f(T_i) = \frac{1}{1+e^{b\_f(T_i - c\_f)}}$	(Chuine, 2000)
M1	This model requires daylength as input variable in addition to daily mean temperature.	$\sum_{t_1}^{DOY} R_f(T_i) \geq (L_i/24)^k F^*$ (4) $R_f(T_i) = \max(T_i - T_c, 0)$	(Blümel and Chmielewski, 2012)
Alternating	Two-phase model that phenological event happens on the first day when forcing is greater than an exponential curve of chilling days.	$\sum_{t_1}^{DOY} R_f(T_i) \geq a + be^{cNCD(t)}$ (5) $R_f(T_i) = \max(T_i - T_c, 0)$	(Cannell and Smith, 1983)
Unichill	Two-phase model using a sigmoid function for chilling accumulates and forcing accumulates, respectively.	$\sum_{t_1}^{DOY} R_f(T_i) \geq F^*$ $\sum_{t_0}^{t_c} R_c(T_j) \geq C^*$ (6) $R_f(T_i) = \frac{1}{1+e^{b\_f(T_i - c\_f)}}$ $R_c(T_j) = \frac{1}{1+e^{a\_c(T_i - c\_c)^2 + b\_c(T_i - c\_c)}}$	(Chuine, 2000)
Sequential	Two-phase model using a triangular response for chilling accumulates, and growing degree days for forcing accumulates.	$\sum_{t_c}^{t_f} R_f(T_d) \geq F^*$ $\sum_{t_0}^{t_c} R_c(T_d) \geq C^*$ $R_f(T_i) = \begin{cases} \frac{1}{1+e^{b\_f(T_i - c\_f)}} \end{cases}$ $R_c(T_j) = \begin{cases} 0 & if\ T_j \leq T_{min} \\ \frac{T_j - T_{min}}{T_{opt} - T_{min}} & if\ T_{min} < T_j \leq T_{opt} \\ \frac{T_j - T_{max}}{T_{opt} - T_{max}} & if\ T_{opt} < T_j \leq T_{max} \\ 0 & if\ T_j \geq T_{max} \end{cases}$ (7)	(Hänninen, 1987)

chilling requirements (C*) during the endodormancy phase (first phase) and the specified total forcing requirements (F*) during the eco-dormancy phase (second phase) (Chuine et al., 1999). Similarly, chilling and forcing accumulate with rates of chilling (R_c) and forcing (R_f) from a fixed date t_0, respectively. Accordingly, apple first flowering and fruit-setting stages are triggered when the cumulative sums of chilling and forcing are greater than or equal to the values of C* and F* . The Alternating model has a variable number of required forcing units that are defined as a function of the total number of days below 0 °C since January 1 (number of chill days, NCD) (Taylor et al., 2018). The Unichill model and Sequential model differ from each other by their temperature response functions for chilling accumulation during the endodormancy phase. A brief introduction was given for each phenological model and the corresponding temperature response functions in Table 1. Additionally, the model parameter descriptions and initial settings were provided in Table 2.

2.4. Model calibration and validation

To calibrate and validate the seven apple phenology simulation models, we pooled the total observation data of apple first flowering and fruit-setting dates from the ten phenology observation sites into a dataset, respectively. Then, we randomly reserved 30% of this pooled dataset for model validation and used the remaining 70% data for model calibration (Step I in Fig. 2). The calibration and validation of each model were conducted based on the differential evolution algorithm in 'scipy' package (version 1.0.0) of the Python language (Storn and Price, 1997). The algorithm minimized the root mean square error (RMSE; Eq. 8) between the observations of apple phenophase and the corresponding model predictions. At first, the model parameters were set in their initial ranges (Table 2). Then, the optimizer was run for 100 iterations to tune the algorithm and ensure convergence. Finally, for each phenological model, the optimal parameter values were selected according to the minimum RMSE value between the observed and predicted blossom/fruit-setting dates in the processes of model calibration and validation.

$$RMSE = \sqrt{\frac{\sum_{i=1}^{n}(O_i - P_i)^2}{n}} \tag{8}$$

where P_i and O_i represent the model-predicted and observed phenological dates (DOY) in year i; and n is the number of observations.

Table 2
Description and initial value ranges of the parameters in the seven apple phenology simulation models.

Parameters	Description	Units	Value range
F*	Total heat forcing requirements	Deg•days	(1000, 2000)
C*	Total chilling requirements	Deg•days	(600, 2000)
T_i	The response temperature to forcing of the Julian day i	℃	(0, 40)
T_j	The response temperature to chilling of the Julian day j	℃	(−40, 16.8)
β_1	Intercept of the linear regression model	-	(−67, 298)
β_2	Slope of the linear regression model	-	(−25, 25)
k	Daylength coefficient (adjusts the total forcing accumulation according to day length)	-	(0, 50)
T_c	Critical temperature	℃	(0, 10)
T_{min}	The minimum temperature for chilling accumulation	℃	(−40,2)
T_{opt}	The optimum temperature for chilling accumulation	℃	(−15,15)
T_{max}	The maximum temperature for chilling accumulation	℃	(5,16.8)
t_0	The DOY (Day of year) on which chilling accumulation begins	DOY	(−67, 298)
t_1	The DOY (Day of year) on which forcing accumulation begins	DOY	(−67, 298)
a	Intercept of the chilling day curve	-	(−1000, 1000)
b	Slope of the chilling day curve	-	(0, 5000)
c	Scale parameter of the chilling day curve	-	(−5, 0)
b_f	Sigmoid function parameter for forcing	-	(−20, 0)
c_f	Sigmoid function parameter for forcing	-	(−50, 50)
a_c	Sigmoid function parameter for chilling	-	(0, 20)
b_c	Sigmoid function parameter for chilling	-	(−20, 20)
c_c	Sigmoid function parameter for chilling	-	(−50, 50)

2.5. Model ensemble

We then integrated these seven calibrated apple phenological models into a model ensemble. Model ensembling is a precedure to combine the predictions of several phenological models to improve the generalizability and robustness of model outputs over those of any single model. Usually, the model ensemble was believed to outperform any member of the integrated models due to its lower variance (Dai et al., 2022). A more detailed process about model ensemble projection was provided in the research framework (Step II in Fig. 2). In this study, we tried to integrate a set of well-performing models to balance out their individual weaknesses and produce more robust prediction results. The weights (w_m) of the member of this model ensemble were not equal, which were determined by the RMSE values of the individual models involved in the process of model validation (Eq. 9). We determined the weight by RMSE values for each participating models in model validation. Thus, the final simulated apple first flowering and fruit-setting dates were actually weighted ensembles of seven different models.

$$w_{\mathrm{m}} = \frac{1}{m_{RMSE} \cdot \sum \frac{1}{\mathrm{m}_{RMSE}}} \tag{9}$$

where w_m is the weight coefficient; m_{RMSE} is the RMSE value of participating model (m).

2.6. Ensemble predictions of apple first flowering and fruit-setting dates

When the model ensemble was driven by daily weather data in the baseline period, the first flowering and fruit-setting dates of apple trees were predicted according to Eq. (10). When the model ensemble was driven by future climate data in the near future and far future, the final phenological predictions were derived according to Eq. (11).

$$DOY_{\mathrm{sim\_baseline}} = \sum_{\mathrm{m}=1}^{7} w_m DOY_m \tag{10}$$

$$DOY_{\mathrm{sim\_future}} = \frac{1}{27}\sum_{n=1}^{27}\sum_{\mathrm{m}=1}^{7} w_m DOY_{n,m} \tag{11}$$

where $DOY_{\mathrm{sim\_baseline}}$ and $DOY_{\mathrm{sim\_future}}$ is the predictions of apple first flowering/fruit-setting dates in the baseline and future period, respectively; n is the number of global climate models (GCMs); m is the number of phenology models; and w is the weight of the ensemble member.

Then, the differences between the first flowering and fruit-setting dates (defined as the phenological sensitive windows in this study) were calculated to track the duration from apple first flowering to fruit-setting. For the sake of simplicity, we analyzed the change of apple phenological sensitive windows with the probability density curves.

2.7. Analysis of late-spring frost risk and climatic risk of poor pollination during apple phenological sensitive windows

2.7.1. Indices of late-spring frost risk

A threshold of 0 °C in air temperature (T_h, commonly measured at

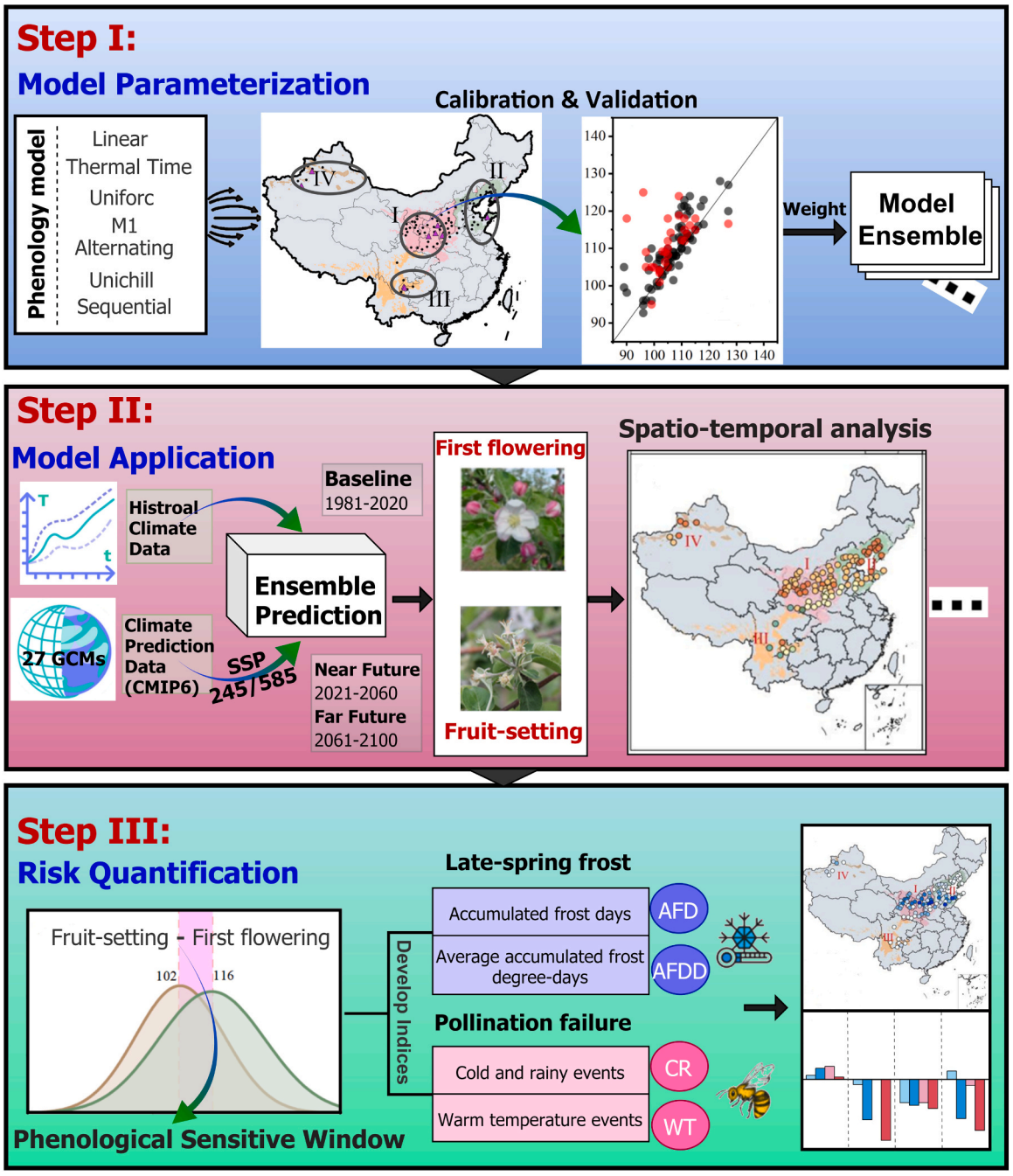

Fig. 2. Research framework of this study.

Table 3
Quantitative indices of late-spring frost risk and climatic risk of poor pollination for *'Fuji'* apple trees in China.

Symbol (unit)	Index	Implication	Equation
AFD (d)	Accumulated frost days	The frequency of frost events	$AFD = \sum_{blossom}^{fruitset} \text{Frost}days_{(T_{min}<T_h)}$ (12)
AFDD (°C d d^{-1})	Average accumulated frost degree-days	The intensity of frost events	$AFDD = \frac{\sum_{blossom}^{fruitset} Max(T_h - T_{min}, 0)}{fruitset - first\ \ flower}$ (13)
CR (%)	Cold and rainy events	The restricted extent of pollination activity	$CR = \frac{\sum_{blossom}^{fruitset} Cold\ \ and\ \ rainy\ \ days_{(T_{max}<12, rain>10)}}{fruitset - first\ \ flower}$ (14)
WT (%)	Warm temperature events	The restricted extent of pollen germination and pollen tube growth rate	$WT = \frac{\sum_{blossom}^{fruitset} Warmdays_{(T_{max}>29)}}{fruitset - first\ \ flower}$ (15)

Note: T_h is the temperature threshold; T_{min} and T_{max} are the daily minimum and maximum air temperature, respectively.

2 m above soil surface) was used to define late-spring frost events for *'Fuji'* apple trees. This measurement was derived from the standard of "*Grade of florescence freezing injury to 'Fuji' apple*" (QX/T 392–2017) issued by the China Meteorological Administration. The indices of accumulated frost days (AFD; Equation 12) and average accumulated frost degree-days (AFDD; Equation 13) were calculated during apple phenological sensitivity windows (Table 3). The index of AFD was defined as the accumulated days when the daily minimum air temperature was below T_h, accounting for the frequency of frost event (Xiao et al., 2018). The other index of AFDD were defined as the average value of the cumulative temperature lower than T_h throughout the phenological sensitivity window, accounting for the intensity of frost event (Deng et al., 2020).

2.7.2. Indices of climatic risk of poor pollination

Successful fruit setting of apple trees relies on the transfer of pollen from external sources as apple flowers are not self-fertile (Yoder et al., 2009). Many weather components such as temperature, rain, fog, and wind speed can affect apple pollination. The optimal air temperature for bee activity was between 15 – 26 °C. There was no bee activity when temperatures are below 10 – 12 °C (Lorite et al., 2020). Bees also stop pollination activity in periods with fog, rain, or wind speed higher than 24 km h^{-1}. Due to the limitations of future climate data related to fog and wind speed obtained from the GCMs, we considered the combination of low temperature and rainfall events (referred as cold and rainy events, CR) as a proxy index. The index of CR (Equation 14) was defined as the accumulated days when the daily maximum air temperature was below 12 °C or the precipitation was higher than 10 mm. In addition, the excessive warm temperature higher than 29 °C (referred as warm temperature event, WT) can also affect apple pollen germination and pollen tube growth rate (Yoder et al., 2009). Thus, the index of WT (Equation 15), defined as the accumulated days for daily maximum air temperature above 29 °C, was also taken into account (Table 3). Based on the two sets of indices above, the late-spring frost risks and the climatic risks of poor pollination during apple phenological sensitivity windows were quantitatively analyzed in the four apple-producing sub-regions of China under future climate warming (Step III in Fig. 2).

3. Results

3.1. Model performance evaluation

3.1.1. Performance of individual phenology models

The values of RMSE were calculated for each individual phenology model in the simulations of apple first flowering dates (Fig. 3a-g) and fruit-setting date (Fig. 4a-g) in the processes of model calibration and validation. The RMSE value ranges were 2.56 – 5.30 d and 3.18 – 7.96 d for apple first flowering dates in the calibration and validation processes, respectively (Fig. 3a-g). Similarly, they were 2.79 – 4.74 d and 3.51 – 5.19 d for apple fruit-setting dates in the calibration and validation processes, respectively (Fig. 4a-g). The average simulation errors of fruit-setting dates were smaller than those of first flowering dates in both calibration and validation processes. For first flowering date (Fig. 3a-g), the Thermal Time and M1 models showed the highest

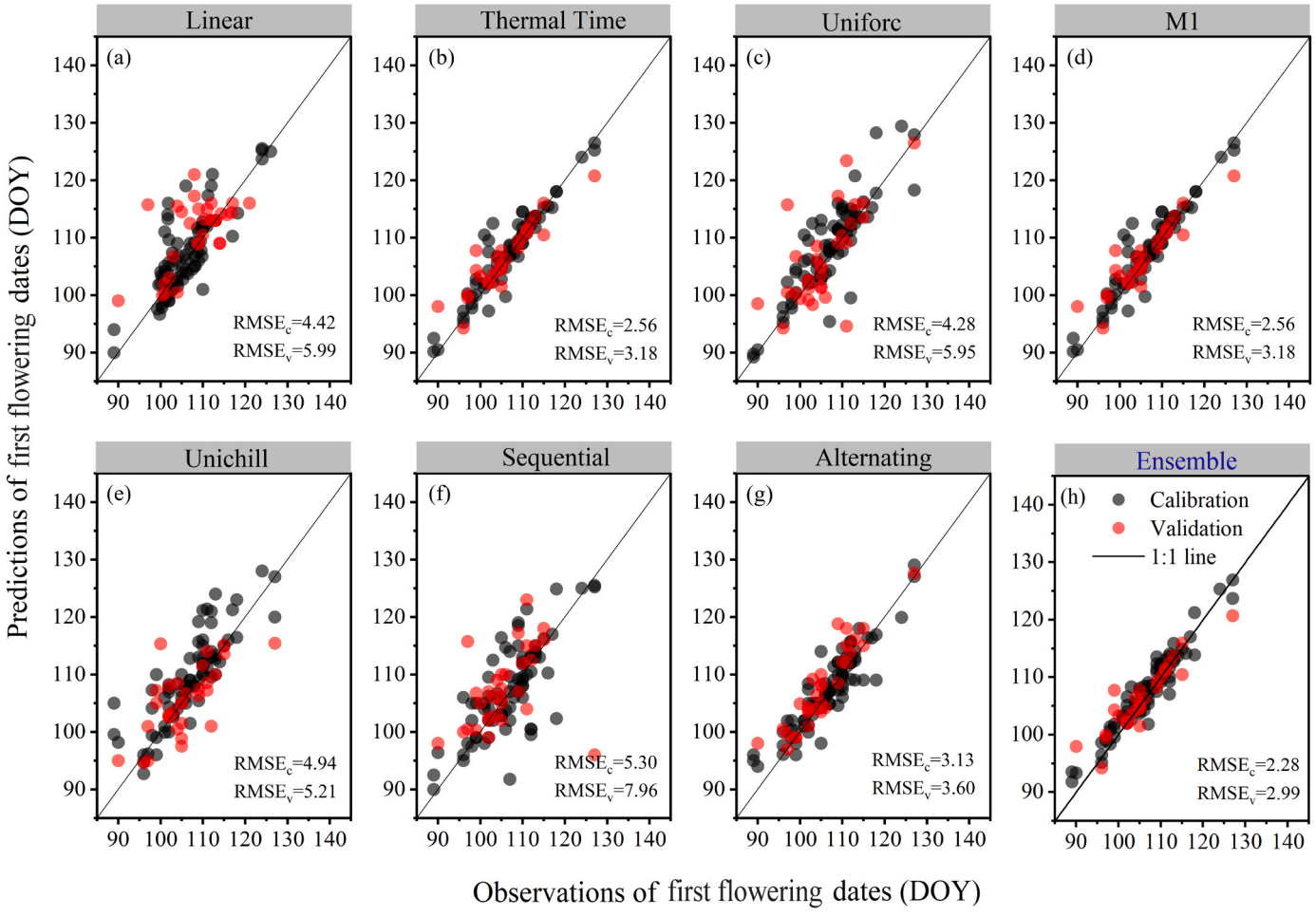

Fig. 3. Root mean square errors (RMSE) between observations and predictions of apple first flowering dates in the process of model calibration (black dots; $RMSE_c$) and model validation (red dot; $RMSE_v$) for each phenology model (a-g) and model ensemble (h). The black solid line is the 1:1 line.

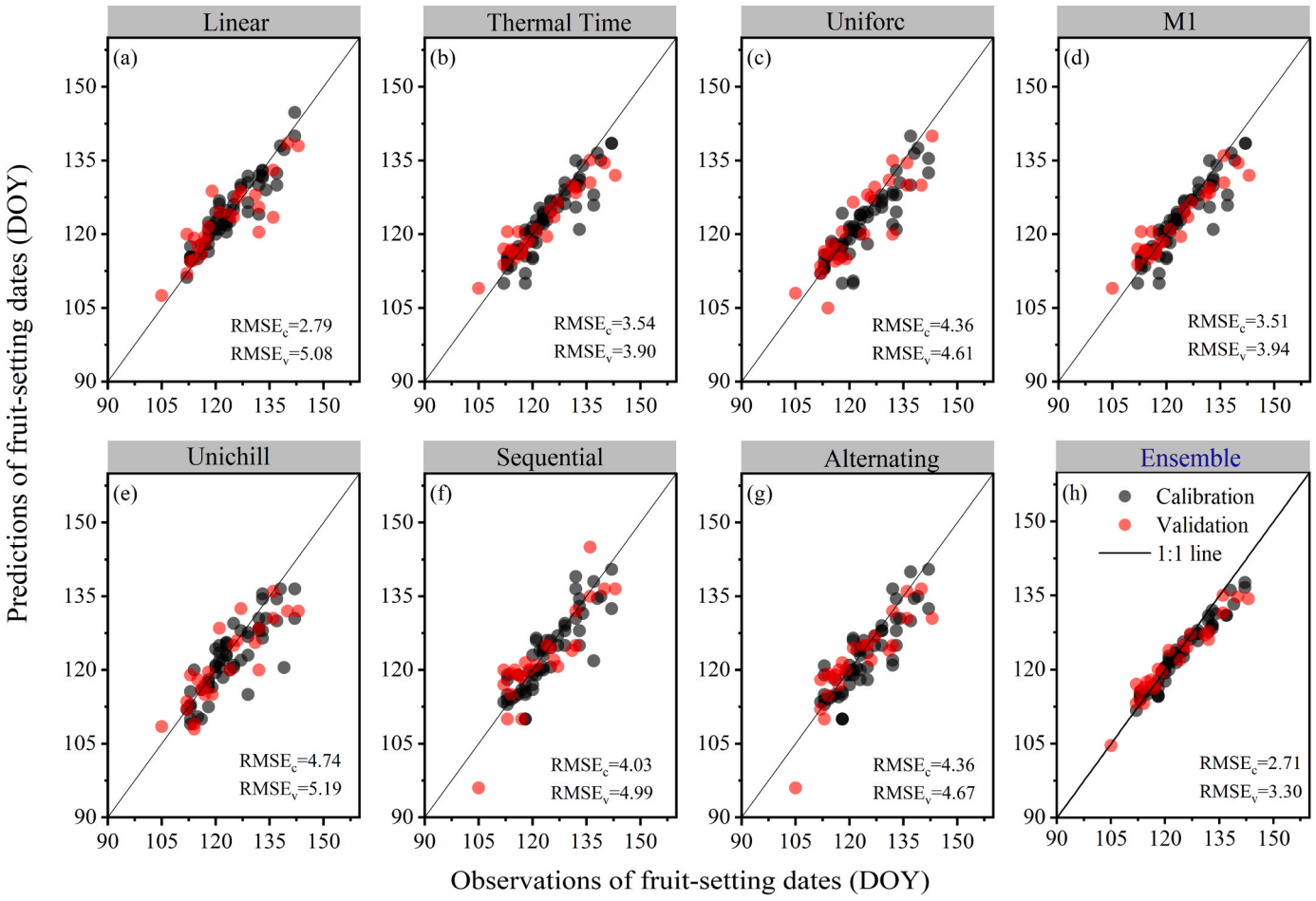

Fig. 4. Root mean square errors (RMSE) between the observations and predictions of apple fruit-setting dates in the process of model calibration (black dots; $RMSE_c$) and model validation (red dot; $RMSE_v$) for each phenology model (a-g) and model ensemble (h). The black solid line is the 1:1 line.

prediction accuracy, with errors less than 3.18 d in calibration and validation processes. The performance of Thermal Time was similar to the M1 model with daylength correction. The performance of the Alternating model followed the above two models, with RMSE values of 3.13 and 3.60 d in the calibration and validation processes. And the RMSE values of the Linear, Uniforc, and Unichill models were all less than 4.94 d and 5.99 d in the calibration and validation processes, respectively. The Sequential model provided relatively more accurate predictions (RMSE=5.30 d) in model calibration, but the errors were up to 7.96 d in model validation. For fruit-setting date (Fig. 4a-g), the Linear model had the lowest error (RMSE=2.79) in the calibration process, while the Thermal Time model provided the smallest error (RMSE=3.90) in the validation process. Notably, there were only slight differences between the M1 and Thermal Time models in fruit-setting date predictions. The RMSE values of M1 and Thermal Time models were 3.94 d and 3.90 d in model validation. And the RMSE values of the other models (including the Uniforc, Unichill, Sequential, and Alternating) were all less than 5.19 d in both processes of model calibration and validation. Generally, the RMSE values of apple first flowering and fruit-setting dates were smaller in the process model calibration than in the process of model validation.

3.1.2. *Performance of model ensemble*

The performances of the ensemble of seven different phenology models were also evaluated for the simulations of apple first flowering and fruit-setting dates (Fig. 4h and Fig. 4h). The RMSE values of the model ensemble were 2.28 d and 2.99 d for the simulaitons of apple first flowering dates in the calibration and validation processes. Similarly, the RMSE values of the model ensemble were 2.71 d and 3.30 d for the simulaitons of apple fruit-setting dates in the calibration and validation processes, respectively. Compared with any individual phenology model, the model ensemble improved the prediction accuracies by 11.04 – 56.95% for apple first flowering dates and by 3.03 – 42.79% for apple fruit-setting dates in the process of model calibration. Similarly, the model ensemble improved the prediction accuracies by 5.97 – 62.42% for apple first flowering dates and by 15.45 – 36.41% for apple fruit-setting dates in the process of model validation. In general, the model ensemble could greatly improve the simulation accuracy for the two phenological stages of apple trees.

3.2. *Changes of apple first flowering and fruit-setting dates*

3.2.1. *Phenological change in the baseline periods*

The temporal and spatial variations of apple first flowering and fruit-setting dates in the baseline period (1980–2020) were shown in Fig. 5. The earliest first flowering date was 68 DOY and the latest was 125 DOY. The earliest fruit-setting date was 73 DOY and the latest was 145 DOY in the four apple-growing sub-regions of China. The general average blossom and fruit-setting dates were 103 and 115 DOY, respectively. Apple first flowering and fruit-setting dates tended to be postponed from south to north in China in the baseline period. Generally, the occurrence of apple phenology was always earlier in southeast region than in northwest region in the baseline period. For instance, apple phenological stage occurred the earliest in Sub-region III, but the latest in Sub-region IV.

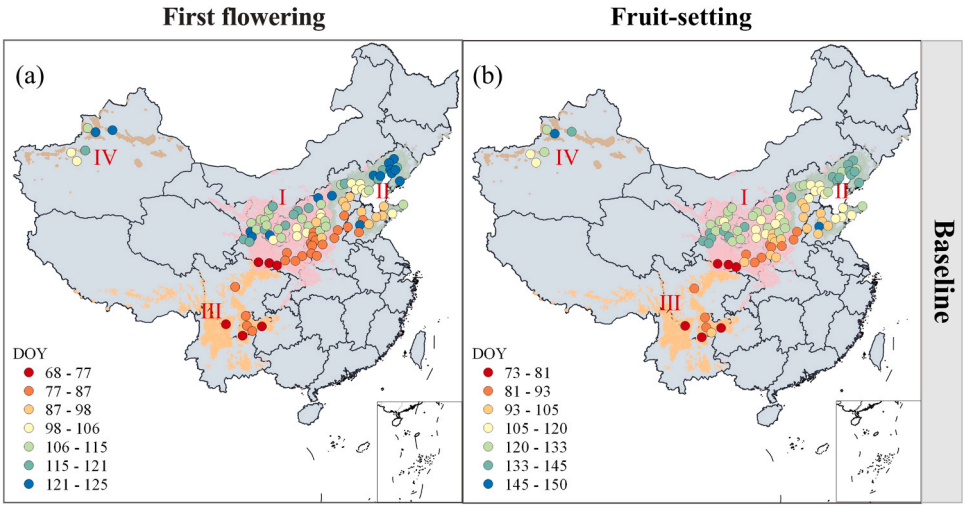

Fig. 5. Spatial distrubitons of apple first flowering (a) and fruit-setting (b) dates projected by the ensemble of multiple phenology models in the baseline period (1981–2020) in the four main apple-growing sub-regions (Sub-region I: the Loess Plateau, II: the Bohai Bay, III: the Southwest Cool Highland, and IV: Xinjiang) of China.

3.2.2. *Phenological change under future climate warming*

Under the two future climate scenarios of SSP245 and SSP585, apple first flowering and fruit-setting dates all became earlier in the four sub-regions (Fig. 6 and Fig. S1). Under SSP245 scenario, the average apple first flowering dates advanced about 7.60 d in the near future (2021–2060) and 12.91 d in the far future (2061–2100) compared with the baseline period (1980–2020); and average fruit-setting dates advanced 9.48 d and 18.60 d, respectively. Compared with the baseline period, about 95% of the representative apple-growing sites had earlier first flowering dates and about 95 – 98% of the sites had earlier fruit-setting dates in the future. However, these two phenological stages could also be delayed sometimes, which mainly occurred under warmer scenarios in low-latitude regions (e.g., the southern edge of Sub-regionI and Sub-region III). Generally, the two phenological dates advanced or delayed greater under SSP585 than under SSP245, especially in the far future period. For instance, the maximum advancing of apple fruit-seting date was up to 29 d, while the maximum delay was up to 31 d under SSP585. Additionally, apple first flowering\fruit-setting dates advanced faster in high-lattidue region (e.g., Sub-region IV, or Xinjiang) than in low-lattitude region (e.g., Sub-region III, or the Southwest Cool Highland). This phenomenon was more obvious when under the warmer scenario of SSP585. For example, the average apple first flowering dates in Sub-region IV advanced about 8.6 d under SSP245, but the average apple first flowering dates in Sub-region I delayed about 16.44 d when under SSP585 in the near future (Fig. S1). Except for Sub-region III, the average advancing of first flowering and fruit-setting dates in near future (2021–2060) was smaller than that in the far future (2061–2100) period under both SSP245 and SSP585 scenarios in the other three sub-regions.

3.3. *Changes in apple phenological sensitivity window*

The changes of phenological sensitivity windows from apple first flowering to fruit-setting dates were analyzed through the probability density curves (Fig. 7 and Fig. S2). In the baseline period, the first flowering and fruit-setting dates of April 12 (102 DOY) and April 26 (116 DOY) were at the maximum probability density, respectively. This means the phenological sensitivity window was about 14 d or two weeks (Fig. 7). However, the phenological sensitivity window became about 10 d under SSP245 and 6 – 9 d under SSP585, respectively, which were much shorter than in the baseline period. Compared with SSP245, the phenological sensitivity window was shortened even more largely under SSP585. Spatially, similar changes of phenological sensitivity windows were found in Sub-regions I and II both under SSP245 and SSP585 (Fig. S2). For instance, the phenological sensitivity windows decreased about 3 – 4 d under SSP245 and reduced 2 – 6 d under SSP585 from about 12 d in Sub-region I and 13 d Sub-region II in the baseline period. It was noteworthy that the phenological sensitivity window in Sub-region III decreased slightly first (about 1 d) and then increased (about 3 –12 d) under the two emission scenarios. In Sub-region IV, the phenological sensitivity window decreased about 3 – 8 d under the two emission scenarios.

3.4. *Late-spring frost risk and climatic risk of poor pollination*

3.4.1. *Risks in the baseline period*

The risks of late-spring frost in apple phenological sensitivity windows, which were represented by the indices of AFD and AFDD, were calculated in the baseline period (Fig. 8a, b). The values of AFD and AFDD were about 0 – 3.59 d and – 0.82 – 0 ℃ d d^{-1} in the baseline period in Sub-regions I and II, respectively. However, there was hardly any frost risk in Sub-region III (with AFD of 0 –0.56 d and AFDD of –0.09 –0 ℃ d d^{-1}) and Sub-region IV (with AFD of 0 –2.08 d and AFDD of –0.23 –0 ℃ d d^{-1}) in the baseline period.

In addition, the values of indices of CR and WT, which were associated with the climatic risk of poor pollination, showed opposite spatial distributions in the baseline period (Fig. 8c, d). The CR values greater than 60% were concentrated in Sub-region III and the southern edge of Sub-regions I and II; the WT values greater than 60% were mainly in Sub-region IV and the northern edges of Sub-regions I and II. This suggested that the climatic risk of poor pollination would occur only in some marginal apple-growing areas in China in the baseline period.

3.4.2. *Changes in late-spring frost risk under future climate warming*

According to the spatial variations of late-spring frost risks under the scenarios of SSP245 and SSP585 (Fig. 9), the change ranges of AFD and AFDD were – 2.85 – 1.88 d, and – 0.89 – 0. 72 ℃ d d^{-1}, respectively. Compared with the baseline period, the sptial changes in AFD and AFDD did not show a consistent spatial pattern under the two scenarios. Under the emission scenario of SSP245, the average changes of AFD and AFDD in all sub-regions were – 0.008 d and – 0.05 ℃ d d^{-1} in the near future, and – 0.12 d and – 0.13 ℃ d d^{-1} in the far future. Under SSP585, the average changes of AFD and AFDD in all sub-regions were – 0.005 d and – 0.10 ℃ d d^{-1} in the near future, and – 0.25 d and – 0.16 ℃ d d^{-1} in the far future, respectively. This indicated that the overall frost risks (represented by frost frequency and intensity) would remain the same or

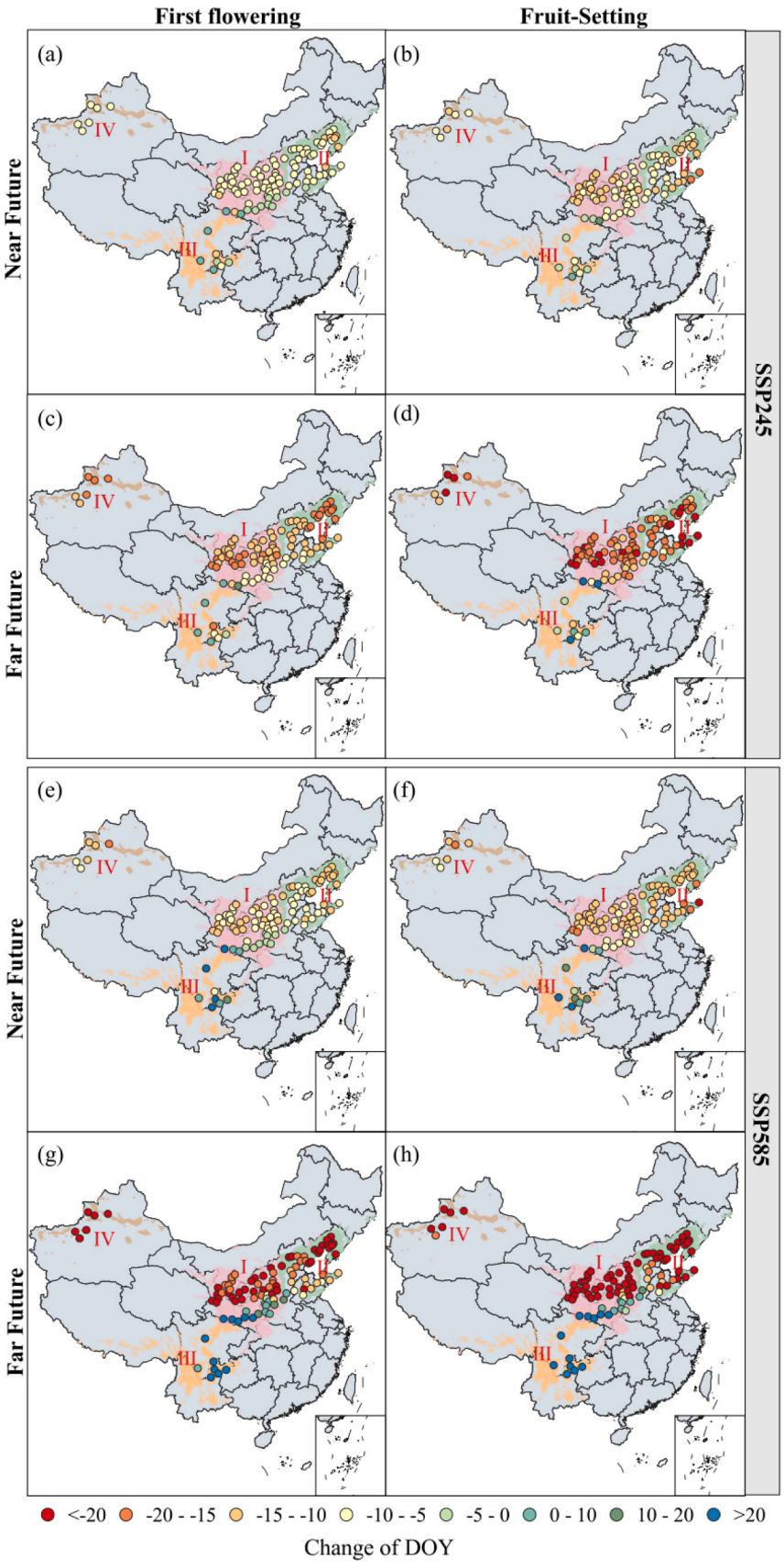

Fig. 6. Spatial distributions of changes of apple first flowering and fruit-setting dates (day of year, DOY) in near future (2021–2060) and far future (2061–2100) projected by the apple phenology model ensemble under the SSP245 and SSP585 scenarios in four main apple-growing subregions (Sub-region I, the Loess Plateau; II, the Bohai Bay; III, the Southwest Cool Highland; and IV, Xinjiang) of China. Changes of apple first flowering and fruit-setting dates were defined as the differences of projected dates between the baseline period (1981–2020) and the two future periods (near future, 2021–2016; far future, 2061–2100) under two emission scenarios of SSP245 (a, b, c, d) and SSP585 (e, f, g, h). Negative values represent the advancing of apple phonological dates, while positive values the delay of apple phonological dates.

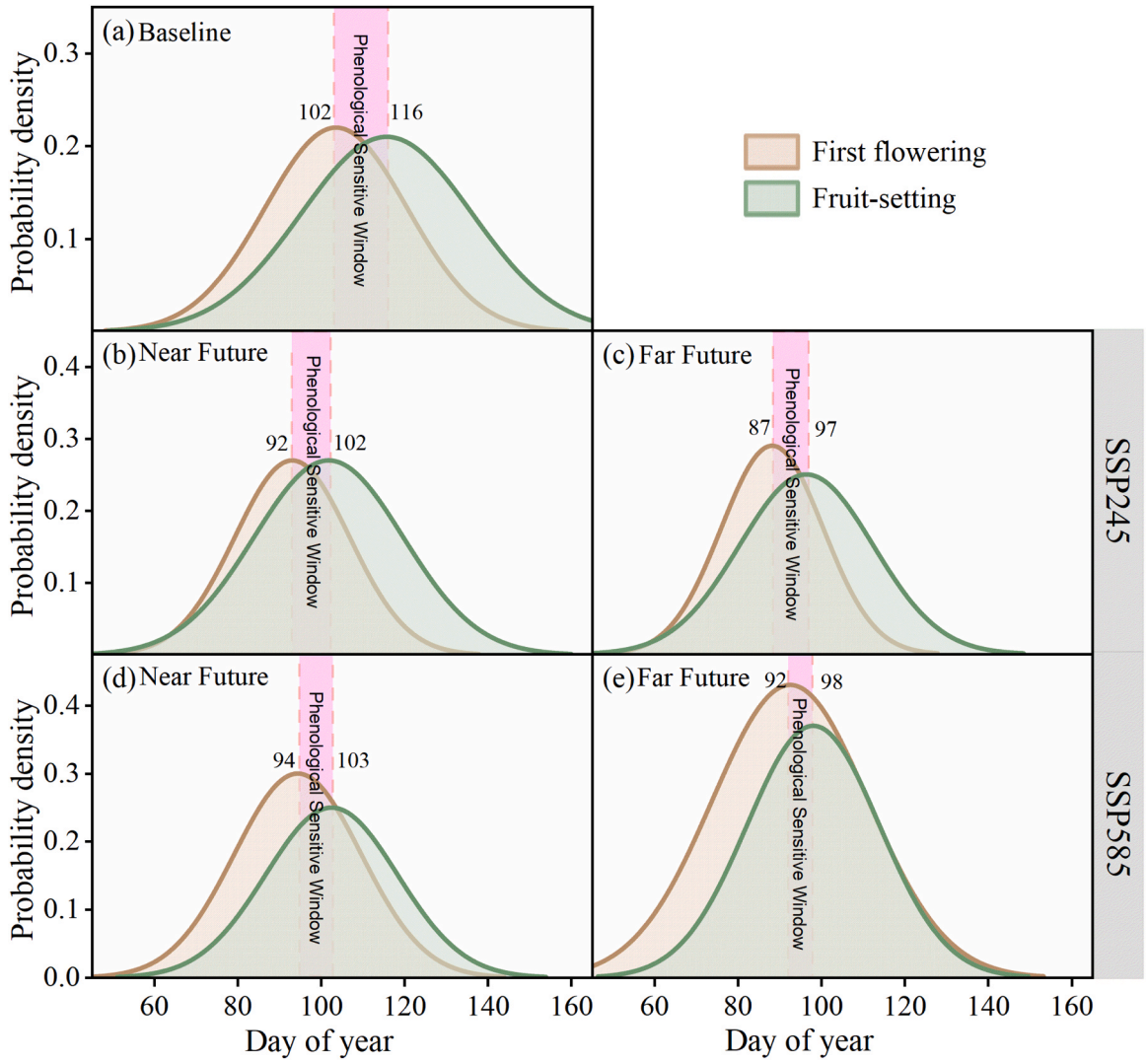

Fig. 7. Probability density curves of first flowering and fruit-setting dates in the baseline period (a), the near future (b, d), ad the far future (c, e) under two emission scenarios of SSP245 and SSP585. The pink rectangular ribbons represent the apple phenological sensitive windows, which are defined as the differences between the first flowering dates and fruit-setting dates at the maximum probability density.

weakly decline in China under future climate warming. However, the comparisons among the four main apple-growing sub-regions did not demonstrate a consistently stable or declining trend in the general pattern of frost risks (Fig. 9 and Fig. S3).

In Sub-region I, the average values of AFD and AFDD increased about 0.02 – 0.13 d y^{-1} and 0.10 – 0.26 ℃ d d^{-1} y^{-1} under the two scenarios, respectively (Fig. S3). In Sub-region II, the average values of AFD decreased about 0.05 – 0.62 d y^{-1}, but the average values of AFDD increased 0.02 – 0.12 ℃ d d^{-1} y^{-1} under the two scenarios. In Sub-region III, the average values of AFD and AFDD decreased about 0.24 – 0.30 d y^{-1} and 0.02 – 0.03 ℃ d d^{-1} y^{-1} under the two scenarios, respectively. In Sub-region IV, the average values of AFD decreased about 0.06 – 0.52 d y^{-1}, but the average values of AFDD increased about 0.07 – 0.36 ℃ d d^{-1} y^{-1}. The results showed that frost frequency and intensity were expected to become lighter in Sub-region III. However, frost frequency and intensity would be more severe in Sub-region I. Although frost events would be less frequent in Sub-region II and IV, the intensity of frost event would be more severe. It was noteworthy that AFD was expected to play a leading role in the change of frost risks in Sub-region II due to the weak increase of AFDD. Thus, the general frost risks in Sub-region II were expected to decline eventually. In addition, in all of the four sub-regions, the decrease of AFD value in the far future was greater than that in the near future period, while the increase of AFDD value in the far future period was greater than that in the near future period both under the two scenarios of SSP245 and SSP585.

3.4.3. Changes in climatic risk of poor pollination under future climate warming

According to the spatial variations of climatic risks of poor pollination under the two emission scenarios of SSP245 and SSP585 (Fig. 10), the changes of CR and WT were about – 10% and 10% of most apple-growing sites in the four sub-regions in China. For instance, the variations of CR and WT were about – 10 – 10% at about 73 – 87% of representative sites in four sub-regions under SSP245 (Fig. 10a-d), while at about 78 – 92% of representative sites in four sub-regions under SSP585 (Fig. 10e-h). This indicated minor changes in climatic risk of poor pollination for apple trees across most representative sites in China. Increase of CR greater than 10% was mainly distributed in the sites of Sub-regions I and II in the far future under the two scenarios. On the contrary, decrease of CR less than – 10% was sporadically distributed in Sub-region III and southern parts of Sub-regions I and II.

In addition, we analyzed the average changes of CR and WT in the four apple-growing sub-regions (Fig. S4). In Sub-region I, the average values of CR and WT increased about 0 – 5% and 2 – 7% under the two

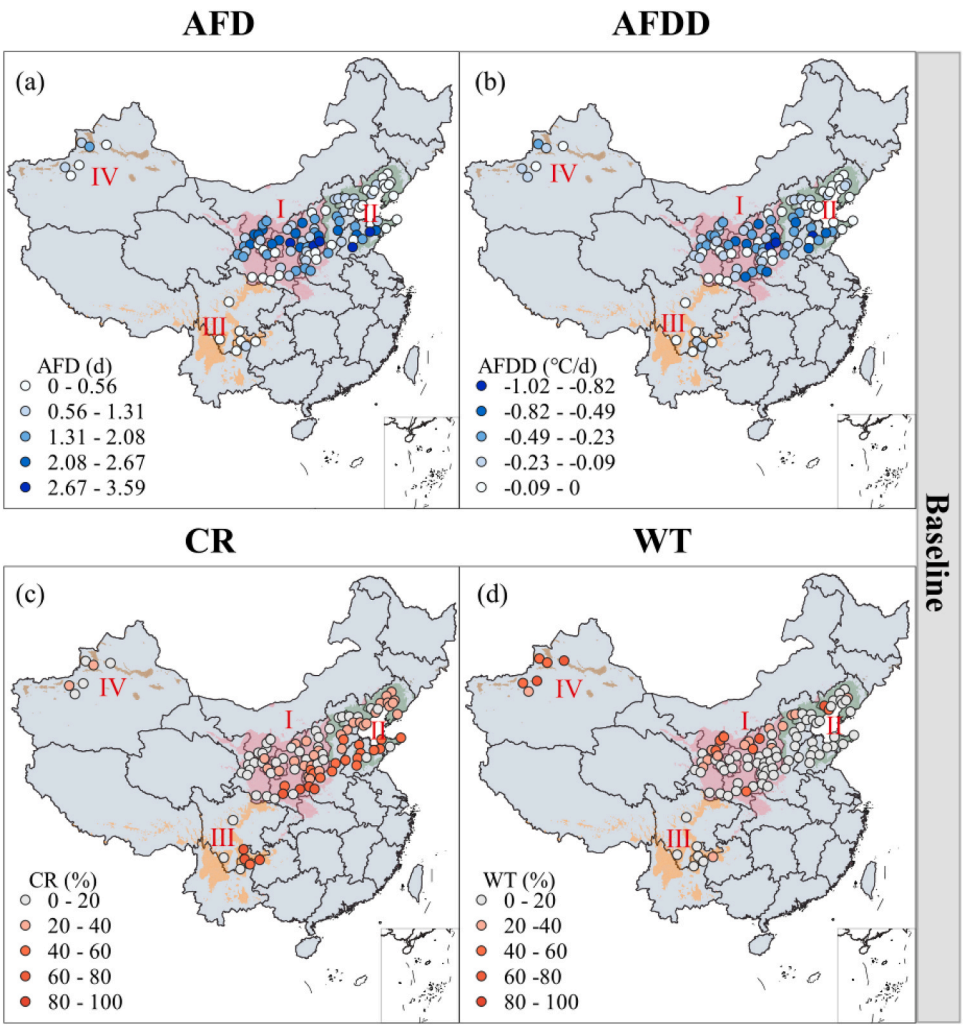

Fig. 8. Spatial distributions of late-spring frost risks and climatic risks of poor pollination in the baseline period (1981 −2020) in four main apple-growing sub-regions (Sub-region I, the Loess Plateau; II, the Bohai Bay; III, the Southwest Cool Highland; and IV, Xinjiang) of China. Frost frequency was represented by the accumulated frost days (AFD, d; a) and frost intensity by the average accumulated frost degree-days (AFDD, ℃ d d^{-1}; b), respectively. Climatic risk of poor pollination was represented by the cold and rainy events (CR, %; c) and the warm temperature events (wt%; d), respectively.

scenarios, respectively. In Sub-region II, the average values CR and WT increased about 0 − 3% and 1 − 2%, except for the far future under SSP585 in which CR decreased about 1%. In Sub-region III, the average values of CR and WT increased about 8 − 30% and 3 − 27% under the two scenarios. In Sub-region IV, the average values of CR decreased about 0 − 2%, except for the near future under SSP245 in which CR increased about 1%. The average values of WT increased about 5 − 12%, except for the far future under SSP245 in which CR decreased about 1%. Data analysis indicated that the general average changes of CR and WT values were small in sub-regions I, II, and IV under the two scenarios. As shown on the map (Fig. 10), only a few representative sites in these regions would likely face an increase in the climatic risk of poor pollination. However, Sub-region III may still need to be focused on, as the values of WT and CR tend to increase under the two climate warming scenarios.

4. Discussion

4.1. Merit of model ensemble in apple phenology simulation

In this study, the performance of seven different phenology simulation models and their ensemble were evaluated first to predict the first flowering and fruit-setting dates of apple trees. The RMSE values of model calibration and validation processes showed the superior performance of multi-model ensemble in apple phenology simulations. For the predictions of apple first flowering and fruit-setting dates, the RMSE values of the model ensemble were all less than 3.3 d, which were even less than the RMSE values reported in some previous studies (Darbyshire et al., 2016; Masaki, 2019). Compared with a single phenological model used arbitrarily, the model ensemble proposed in this study could improve the simulation accuracy by about 5.97–62.42% and about 15.45–36.41% for apple first flowering and fruit-setting dates in the validation process, respectively. Our results confirmed that the performance of model ensemble of all single models was slightly better than or comparable to the best single model when predicting certain state variables in some previous studies about crop model comparison (Ruane et al., 2017; Tao et al., 2018). To our knowledge, the use of ensemble methods to improve apple first flowering and fruit-setting date predictions has seldom been reported in the world.

When individual models were compared, the Thermal Time and M1 models included in the one-phase model performed slightly better than other models. And the Alternating model included in the two-phase model performed slightly better than other models. However, the overall performance between one-phase models (including Thermal Time, Uniforc, and M1 model) and two-phase models (including Unichill, Sequential, and Alternating model) was similar in the prediction of apple first flowering/fruit-setting dates according to the RMSE values. This might indicate that the chilling in winter had no major effect on the apple first flowering/fruit-setting date because apple trees could accumulate sufficient chilling to release dormancy under the current observation conditions (Guo et al., 2019; Masaki, 2019; Ru et al., 2023). Consequently, this may also mean that the one-phase models are complex enough to predict apple phenological dates under the current weather conditions. But the two-phase model could provide more

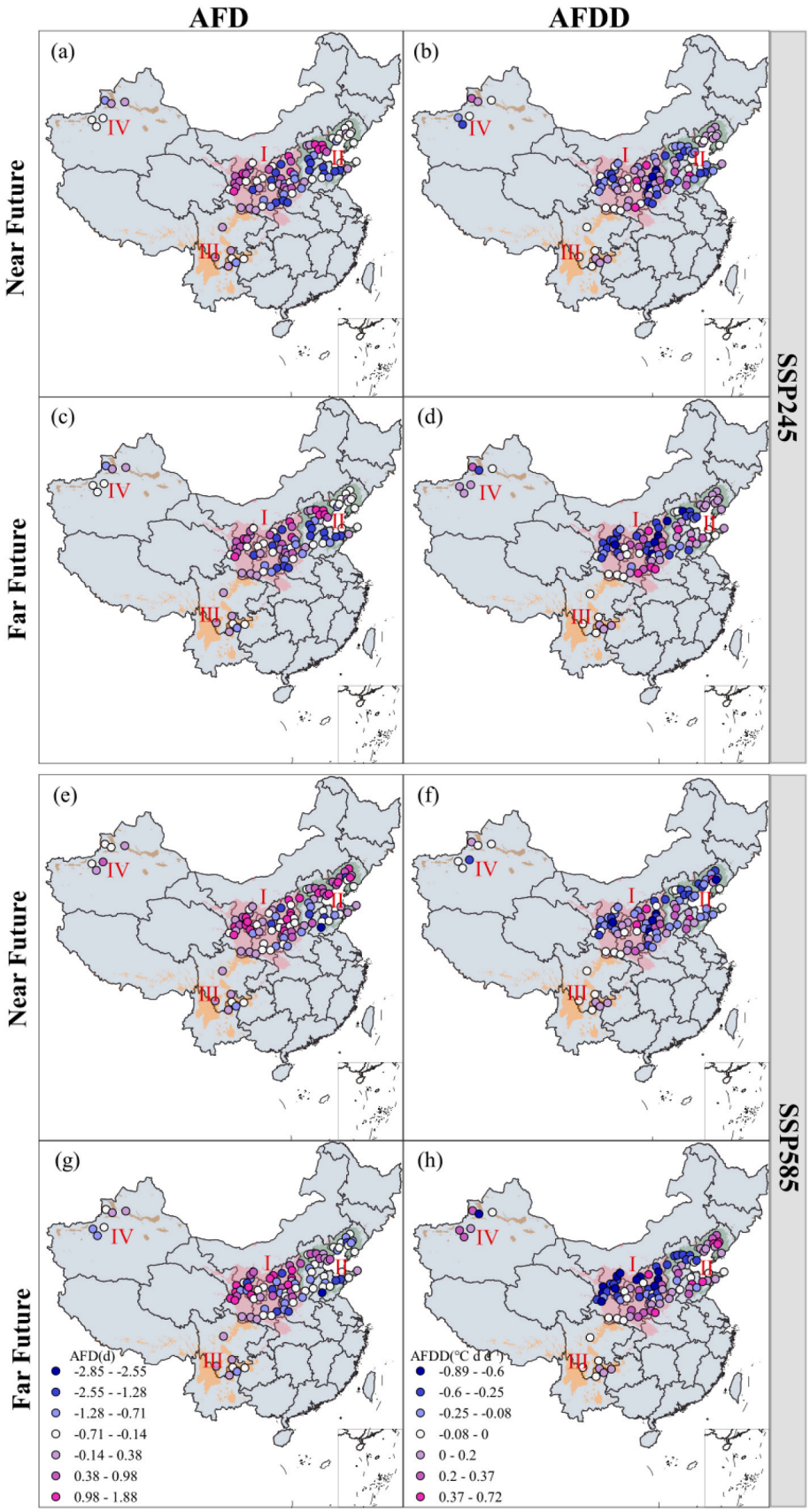

Fig. 9. Spatial distributions of the changes of frost frequency (represented by the accumulated frost days, AFD) and frost intensity (represented by the average accumulated frost degree-days, AFDD) in four main apple-growing sub-regions (Sub-region I, the Loess Plateau; II, the Bohai Bay; III, the Southwest Cool Highland; and IV, Xinjiang) of China in the near future (2021–2060) and far future (2061–2100) under two emission scenarios of SSP245 (a, b, c, d) and SSP585 (e, f, g, h).

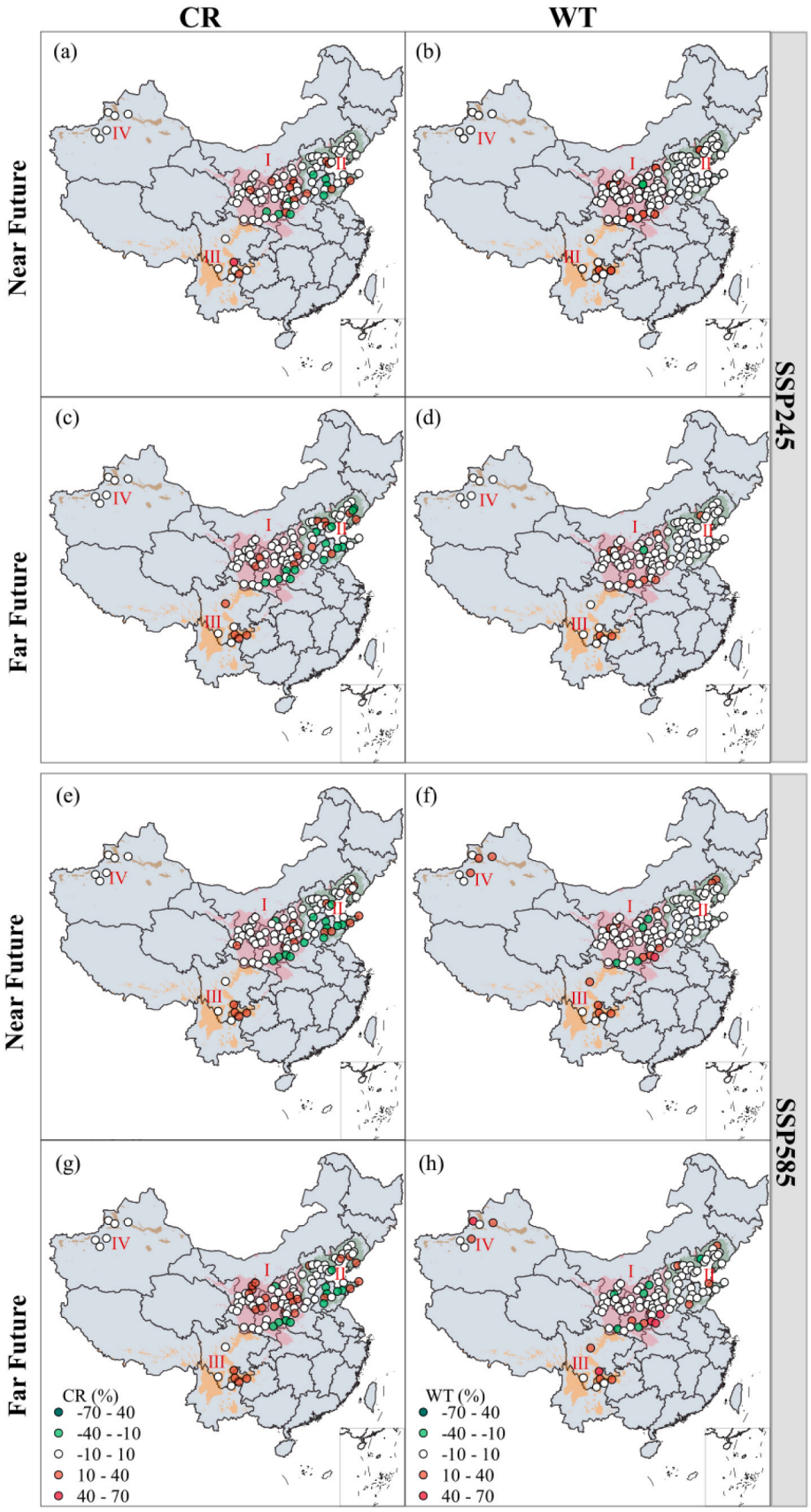

Fig. 10. Spatial distributions of the changes of the cold and rainy events (CR) and the warm temperatures events (WT) in apple phenological sensitive windows in four main apple-growing sub-regions (Sub-region I, the Loess Plateau; II, the Bohai Bay; III, the Southwest Cool Highland; and IV, Xinjiang) of China in the near future (2021–2060) and far future (2061–2100) under two emission scenarios of SSP245 (a, b, c, d) and SSP585 (e, f, g, h).

accurate phenology predictions under future warming climate change (Asse et al., 2020). In addition, we also included a simple statistical model (Linear model) in our model ensemble, which had comparable qualities to other physiological process models. Finally, the ensemble of all available apple phenology simulation models could provide better prediction performance than the best individual model in our study. Phenology predictions with higher accuracy and lower bias could avoid the pitfalls of model selection and greatly help reduce the inherent uncertainties in related simulation studies about climate change.

4.2. Impacts of climate change on apple first flowering and fruit-setting

Similar to the report by Wang et al. (2021) on apple first flowering dates in Shaanxi Province of China, apple first flowering and fruit-setting dates tended to be postponed from southeast to northwest in our study area in the baseline period. This was because the temperature has an obviously incremental trend from the southeast to the northwest in China mainland. Under the two scenarios of future climate warming, the dates of apple blossom and fruit-setting would become earlier. And the advancing followed clear latitudinal and longitudinal gradients overall. These two phenologic dates advanced greater under the emission scenario of SSP585 than under SSP245. The advancing of apple phenophase under future climate warming has been widely reported in Europe (Chmielewski et al., 2018; Legave et al., 2013; Wypych et al., 2017), South Africa (Grab and Craparo, 2011), Japan (Masaki, 2019), Iran (Karami and Asadi, 2017), and Australia (Darbyshire et al., 2013). In this study, we confirmed the advancing of apple first flowering and fruit-setting dates under climate warming in the four apple-growing sub-regions of China as in other regions in the world. The advancing of apple phenophase was due to the fact that after completing chilling accumulation, heat forcing was satisfied prematurely due to the rising temperature. Our results supported that the advancing effect of spring phenology due to warming temperatures during the ecodormancy period exceeded the delaying effect caused by warming during endodormancy (Legave et al., 2015; Pertille et al., 2022). Additionally, the spatial pattern that first flowering\fruit-setting dates advanced faster in high-latitude areas (e.g., Sub-region IV, or Xinjiang) than in low-latitude areas (e.g., Sub-region III, or the Southwest Cool Highland) was more apparent under the warmer scenario of SSP585. This was probably mainly due to the uneven levels of climatic warming across different regions in China. Usually there was a higher or faster temperature rising in high-latitude regions. The first flowering and fruit-setting dates in a few sites of Sub-regions I and III were delayed under the two scenarios. The kind of phenophase delay was probably because the chilling accumulation was limited by the rising temperature and it took longer time than before to complete the chilling requirements to break apple ecodormancy (Fernandez et al., 2022).

4.3. Changes of apple phenological sensitivity windows

Based on the spatial distributions and probability density curves of apple first flowering and fruit-setting dates, the phenological sensitivity windows were calculated for the four apple-growing sub-regions of China. Generally, apple phenological sensitivity windows tended to be shortened in some sub-regions of China, especially under the scenario of SSP585. According to our projections, the apple phenological sensitivity window was about 14 d in the baseline period, but became about 10 d under SSP245 and 6–9 d under SSP585, respectively. This is a very interesting finding seldom reported in related apple studies. Some studies reported that variations in the phenological sensitive window (referred to as 'interphase duration' in their study) of spring phenological events had cascading effects on later phenological events (e.g., maturity phases) in woody plants (Ettinger et al., 2018). This finding inspired us to assume that the shortening of phenological sensitive window would probably cause an earlier ripening of apple fruit. However, our study only assumed this possibility from the perspective of phenology modeling, and a large number of experimental studies are needed to verify this assumption. In addition, unlike other sub-regions, the phenology projection results of Sub-region III or the Southwest Cool Highland showed that the phenological sensitive window was first shortened and then lengthened. Some previous studies on grapevine phenology argued that the variations in phenological sensitive windows (referred to as 'interval length' in their study) had a curvilinear relationship with the daily maximum temperatures in spring (Calò et al., 1994; Cameron et al., 2022). This curvilinear response indicated that the shortening rate of phenological sensitive window would gradually slow down until reach a plateau as the daily maximum temperature increased, and the phenological sensitive window would then lengthen when the daily maximum temperature exceeded the critical point (Calò et al., 1994). Thus, their findings might help explain the nonlinear change of apple phenological sensitive windows in Sub-reigon III.

4.4. Changes of late-spring frost risks and climatic risks of poor pollination

Further analyses were conducted on the late-spring frost risks and climatic risks of poor pollination during the phenological sensitive window of apple trees. For late-spring frost risks, the areas with frequent and severer frost events were mainly concentrated in eastern Gansu, Shaanxi, Shanxi, and Shandong provinces in the baseline period. These areas were basically consistent with the regions that were most often frost-stricken in last decades in China (Qiu et al., 2020; Wang et al., 2020). Compared with the baseline period, frost frequency decreased greater in the far future than in the near future period, while frost intensity increased greater in the far future than in the near future period both under SSP245 and SSP585 scenarios regardless of the sub-regions. This suggested that although the frequency of frost events was expected to decrease, future climate warming would unlikely decrease the intensity of late-spring frosts for apple trees in the second 50 years of the 21st century. This finding aligned with the research conducted by Kunz and Blanke (2022), supporting the notion that frost risk for apple trees continues to exist and may even intensify under climate change. In addition, the overall pattern of late-spring frost risks varied among the four apple-growing sub-regions of China under the two emission scenarios. On average, late-spring frost risks were expected to decrease in Sub-region II (the Bohai Bay) and III (the Southwest Cool Highland) under the two emission scenarios. There was no frost risk in Sub-region III in the baseline period and this sub-region would remain immune to frost risk in future climate warming. However, late-spring frost risks were expected to increase in Sub-region I (the Loess Plateau). The results were less consistent with the findings reported by Guo et al. (2019) about frost risks during apple first flowering stage in Shaanxi province that is mainly located in Sub-region I. They only detected minor frost risks in the past and predicted decreased frost risks with future climate warming. This discrepancy was probably due to the fact that Guo et al. (2019) only used a single phenological model and their results might have large uncertainties in the predictions of apple phenological dates. In Sub-region IV (Xinjiang), late-spring frost risks were expected to be less frequent, but the intensity would become more severe. Thus, more attentions should be focused on the studies on late-spring frost risks in Sub-regions I (the Loess Plateau) and IV (Xinjiang), including the ways to monitor frost risks and facilitate frost interventions.

Based on the two indices CR and WT of climatic risks of poor pollination, the specific meteorological thresholds for bee activities and apple pollen tube growth rates were evaluated in the four main apple-growing sub-regions of China. To our best knowledge, this current research was one of the very few studies that assessed the climatic risks of poor pollination for apple trees in China. According to our results, the climatic risks of poor pollination only occurred in some marginal areas of the four sub-regions in the baseline period. Compared with the baseline period, minor changes ($\pm$ 10%) occurred in climatic risks of poor pollination at most representative sites in the four sub-regions

under the two emission scenarios. Generally, the climatic risks of poor pollination were expected to increase in Sub-region III or Southwest Cool Highland under the two emission scenarios. For the other sub-regions, the climatic risks of poor pollination would increase only at some sites, and these sites might be mainly at the margins of the sub-regions. The increase of climatic risks of poor pollination in Sub-regions III was due to the limited pollen tube growth rate caused by excessive warm events. On the other hand, the activities of pollinators are restricted due to the increase of cold and rainy events during apple phenological sensitive window. A climate-driven timing mismatch between the dates of apple flowering peak and the dates of pollinators (e.g., bees) may be increasing, according to new research from the UK (Wyver et al., 2023). This result expressed a strong concern about apple blossom poor pollination risk. Our results showed that pollination may still be at risk of failure due to climatic conditions (for example in the Southwest Cool Highland of China) from another perspective, even if the phenological dates are matched between pollinators and flowering. Our work provided new insight into the risk of poor pollination due to phenological shifts.

However, we acknowledge that the dynamics of both the frost and poor pollination may be altered because of the differences in phenological dates of specific apple varieties in their responses to climate change. The phenological projections in this study were only based on a single apple variety of 'Fuji', assuming a fixed response of its phenology to different climatic conditions. In fact, different available apple varieties, including cultivars with 'early' or 'late' flower/fruit-setting phenophases, could provide valuable opportunities for the adaptation of apple production to climate change. Thus, it is necessary to collect detailed and long-term phenological data from a wider range of apple varieties, encompassing various growing regions and environmental conditions. With an increased number of observations, we can gain more insights into the underlying natural mechanisms that influence apple phenological processes. Hence, it is necessary to conduct additional researches to enhance the efficacy of current phenological models, as well as to advance the development of novel and intricately precise models founded upon more comprehensive comprehension of apple phenological mechanisms.

5. Conclusions

In this study, an ensemble of seven different apple phenology simulation models driven by climatic data derived from multiple global climate models was used to evaluate the impacts of future climate warming on apple phenology, as well as the risks of late-spring frost and the climatic risks of poor pollination for apple production in China. The four major apple-growing sub-regions of China were wholely covered in our study for the first time. The results showed that the model ensemble could greatly improve the prediction accuracies of apple first flowering and fruit-setting dates, compared with any arbitrarily used single model. The results confirmed the general advancing of apple phenological stages under future climate warming in China. The apple phenological sensitive windows tended to be shortened. And this kind of shortening might indicate that the subsequent apple phenological dates would be advanced (e.g., the harvest date). In addition, this kind of shortening of apple phenological sensitive windows could reduce the frequency of climatic risks in the apple phenological sensitive windows. For instance, the frequency of late-spring frost in Sub-region II (the Bohai Bay), Sub-region III (the Southwest Cool Highland), and Sub-region IV (Xinjiang) of China was expected to decrease on average. However, due to the impacts of increased frost intensity, Sub-region I (the Loess Plateau) and Sub-region IV (Xinjiang) would face higher risks of late-spring frost. Due to lightened frequency and intensity of frost events, Sub-region III would remain immune to frost risks under future climate warming. Finally, shifts in climatic risks of poor pollination were relatively small in China under future climate warming from the perspective of spatial contrasts, except for Sub-region III and a few sites in Sub-regions I and IV. The advanced apple phenology dates lead to divergent trends in late-spring frost riks and climatic risks of poor pollination in the four main apple-growing sub-regions of China. More focus on the climatic risks of poor pollination in Sub-region III and the risks of late-spring frost in Sub-region I and IV are warranted. Generally, our results highlighted the necessity to develop appropriate adaptation measures to avoid late-spring frost risks, rather than climatic risks of poor pollination under future climate change in main apple-growing regions of China.

CRediT authorship contribution statement

Xiaoya Ru: Writing – review & editing, Methodology, Validation, Writing – original draft, Formal analysis, Data processing. **Jie Zhou**: Formal analysis, Investigation. **Kaiyuan Gong:** Data processing, Data curation. **Zhihao He**: Methodology, Formal analysis. **Zhanwu Dai:** Writing – review & editing, Methodology, Supervision. **Meirong Li:** Resources, Methodology. **Xinxin Feng**: Resources. **Qiang Yu**: Methodology, Supervision. **Hao Feng:** Funding acquisition, Supervision. **Jianqiang He**: Methodology, Writing – review & editing, Supervision, Funding acquisition.

Declaration of Competing Interest

The authors declare that they have no known competing financial interests or personal relationships that could have appeared to influence the work reported in this paper.

Data Availability

Data will be made available on request.

Acknowledgements

This research was partially supported by the National Key Research and Development Program of China (No. 2021YFD1900700), the National Natural Science Foundation of China (No. 52079115), the Natural Science Foundation of Shaanxi Province of China (No. 2023-JC-YB-279), the Key Research and Development Program of Shaanxi (No. 2019ZDLNY07-03), and the "111 Project" (No. B12007) of China. The author would like to thank Chinese Meteorological Administration (CMA) for providing the meteorological data.

Appendix A. Supporting information

Supplementary data associated with this article can be found in the online version at doi:10.1016/j.eja.2023.126945.

References

Asse, D., Randin, C.F., Bonhomme, M., Delestrade, A., Chuine, I., 2020. Process-based models outcompete correlative models in projecting spring phenology of trees in a future warmer climate. Agric. . Meteorol. 285–286, 107931 https://doi.org/10.1016/j.agrformet.2020.107931.

Blümel, K., Chmielewski, F.-M., 2012. Shortcomings of classical phenological forcing models and a way to overcome them. Agric. . Meteorol. 164, 10–19. https://doi.org/10.1016/j.agrformet.2012.05.001.

Boyer, W.D., 1973. Air temperature, heat sums, and pollen shedding phenology of longleaf pine. Ecology 54, 420–426. https://doi.org/10.2307/1934351.

Calò, A., Tomasi, D., Costacurta, A., Biscaro, S., Aldighieri, R., 1994. The effect of temperature thresholds on grapevine (Vitis sp.) bloom. An interpretative model. Rivista di Viticoltura e di Enologia (Italy) 47, 3–14.

Cameron, W., Petrie, P.R., Barlow, E.W.R., 2022. The effect of temperature on grapevine phenological intervals: sensitivity of budburst to flowering. Agric. . Meteorol. 315, 108841 https://doi.org/10.1016/j.agrformet.2022.108841.

Cannell, M., Smith, R., 1983. Thermal time, chill days and prediction of budburst in Picea sitchensis. J. Appl. Ecol. 951–963. https://doi.org/10.2307/2403139.

Chapman, P., Catlin, G., 1976. Growth stages in fruit trees-from dormant to fruit set. N. Y. 'S. Food Life Sci. Bull. 58.

Chmielewski, F., Götz, K., Weber, K.C., 2018. Climate change and spring frost damages for sweet cherries in Germany. Int. J. Biometeorol. 62 https://doi.org/10.1007/s00484-017-1443-9.

Cho, J.G., Kumar, S., Kim, S.H., Han, J.-H., Durso, C.S., Martin, P.H., 2020. Apple phenology occurs earlier across South Korea with higher temperatures and increased precipitation. Int. J. Biometeorol. https://doi.org/10.1007/s00484-020-02029-1.
Chuine, I., 2000. A unified model for budburst of trees. J. Theor. Biol. 207, 337–347. https://doi.org/10.1006/jtbi.2000.2178.
Chuine, I., Cour, P., Rousseau, D.D., 1999. Selecting models to predict the timing of flowering of temperate trees: implications for tree phenology modelling. Plant Cell Environ. 22, 1–13. https://doi.org/10.1046/j.1365-3040.1999.00395.x.
Dai, W., Jin, H., Liu, T., Jin, G., Zhang, Y., Zhou, Z., 2022. Applying ensemble learning in ecophysiological models to predict spring phenology. . Ecol. Manag. 505, 119911 https://doi.org/10.1016/j.foreco.2021.119911.
Darbyshire, R., Pope, K., Goodwin, I., 2016. An evaluation of the chill overlap model to predict flowering time in apple tree. Sci. Hortic. 198, 142–149. https://doi.org/10.1016/j.scienta.2015.11.032.
Darbyshire, R., Webb, L., Goodwin, I., Barlow, E.W., 2013. Evaluation of recent trends in Australian pome fruit spring phenology. Int. J. Biometeorol. 57, 409–421. https://doi.org/10.1007/s00484-012-0567-1.
Deng, G., Zhang, H., Yang, L., Zhao, J., Guo, X., Ying, H., Rihan, W., Guo, D., 2020. Estimating frost during growing season and its impact on the velocity of vegetation greenup and withering in Northeast China. Remote Sens 12, 1355. https://doi.org/10.3390/rs12091355.
Drepper, B., Gobin, A., Van Orshoven, J., 2022. Spatio-temporal assessment of frost risks during the flowering of pear trees in Belgium for 1971–2068. Agric. . Meteorol. 315, 108822 https://doi.org/10.1016/j.agrformet.2022.108822.
Eccel, E., Rea, R., Caffarra, A., Crisci, A., 2009. Risk of spring frost to apple production under future climate scenarios: the role of phenological acclimation. Int. J. Biometeorol. 53, 273–286. https://doi.org/10.1007/s00484-009-0213-8.
Ettinger, A.K., Gee, S., Wolkovich, E.M., 2018. Phenological sequences: how early-season events define those that follow. Am. J. Bot. 105, 1771–1780. https://doi.org/10.1002/ajb2.1174.
FAO, 2021. FAOSTAT database. Food and Agriculture Organization of the United Nations. (http://www.fao.org/faostat/en).
Farajzadeh, M., Rahimi, M., Kamali, G.A., Mavrommatis, T., 2010. Modelling apple tree bud burst time and frost risk in Iran. Meteorol. Appl. 17, 45–52. https://doi.org/10.1002/met.159.
Fernandez, E., Schiffers, K., Urbach, C., Luedeling, E., 2022. Unusually warm winter seasons may compromise the performance of current phenology models – predicting bloom dates in young apple trees with PhenoFlex. Agric. . Meteorol. 322, 109020 https://doi.org/10.1016/j.agrformet.2022.109020.
Fraga, H., Santos, J.A., 2021. Assessment of climate change impacts on chilling and forcing for the main fresh fruit regions in Portugal. Front. Plant Sci. 12, 689121 https://doi.org/10.3389/fpls.2021.689121.
Fujisawa, M., Kobayashi, K., 2010. Apple (Malus pumila var. domestica) phenology is advancing due to rising air temperature in northern Japan. Glob. Change Biol. 16, 2651–2660. https://doi.org/10.1111/j.1365-2486.2009.02126.x.
Grab, S., Craparo, A., 2011. Advance of apple and pear tree full bloom dates in response to climate change in the southwestern Cape, South Africa: 1973-2009. Agric. . Meteorol. 151 https://doi.org/10.1016/j.agrformet.2010.11.001.
Gritti, E.S., Duputie, A., Massol, F., Chuine, I., 2013. Estimating consensus and associated uncertainty between inherently different species distribution models. Methods Ecol. Evol. 4, 442–452. https://doi.org/10.1111/2041-210X.12032.
Guo, L., Wang, J., Li, M., Liu, L., Xu, J., Cheng, J., Gang, C., Yu, Q., Chen, J., Peng, C., Luedeling, E., 2019. Distribution margins as natural laboratories to infer species' flowering responses to climate warming and implications for frost risk. Agric. . Meteorol. 268, 299–307. https://doi.org/10.1016/j.agrformet.2019.01.038.
Hänninen, H., 1987. Effects of temperature on dormancy release in woody plants. Silva Fenn. 21, 279–299. https://doi.org/10.14214/sf.a15476.
Hufkens, K., Basler, D., Milliman, T., Melaas, E.K., Richardson, A.D., Goslee, S., 2018. An integrated phenology modelling framework in R. Methods. Ecol. Evol. 9, 1276–1285. https://doi.org/10.1111/2041-210x.12970.
Iovane, M., Cirillo, A., Izzo, L.G., Di Vaio, C., Aronne, G., 2021. High temperature and humidity affect pollen viability and longevity in Olea Europaea L. Agronomy 12 (1). https://doi.org/10.3390/agronomy12010001.
IPCC, 2021: Climate Change 2021: The Physical Science Basis. Contribution of Working Group I to the Sixth Assessment Report of the Intergovernmental Panel on Climate Change [Masson-Delmotte, V., P. Zhai, A. Pirani, S.L. Connors, C. Péan, S. Berger, N. Caud, Y. Chen, L. Goldfarb, M.I. Gomis, M. Huang, K. Leitzell, E. Lonnoy, J.B.R. Matthews, T.K. Maycock, T. Waterfield, O. Yelekçi, R. Yu, and B. Zhou (eds.)]. Cambridge University Press, Cambridge, United Kingdom and New York, NY, USA, In press, https://doi.org/10.1017/9781009157896.
Kalväne, G., Gribuste, Z., Kalväns, A., 2021. Full flowering phenology of apple tree (Malus domestica) in Pūre orchard, Latvia from 1959 to 2019. Adv. Sci. Res. 18, 93–97. https://doi.org/10.5194/asr-18-93-2021.
Karami, M., Asadi, M., 2017. The phenological stages of apple tree in the North Eastern of Iran. Comput. Water Eng. Environ. Eng. 6, 269. https://doi.org/10.4236/cweee.2017.63018.
Kaukoranta, T., Tahvonen, R., Ylämäki, A., 2010. Climatic potential and risks for apple growing by 2040. Agric. Food Sci. 19, 144–159. https://doi.org/10.2137/145960610791542352.
Kunz, A., Blanke, M., 2022. 60 years on"—effects of climatic change on tree phenology—a case study using pome fruit. Horticulturae 8, 110. https://doi.org/10.3390/horticulturae8020110.
Legave, J.M., Farrera, I., Almeras, T., Calleja, M., 2008. Selecting models of apple flowering time and understanding how global warming has had an impact on this trait. J. Hortic. Sci. Biotechnol. 83, 76–84. https://doi.org/10.1080/14620316.2008.11512350.
Legave, J.M., Guedon, Y., Malagi, G., El Yaacoubi, A., Bonhomme, M., 2015. Differentiated responses of apple tree floral phenology to global warming in contrasting climatic regions. Front. Plant Sci. 6, 1054–1067. https://doi.org/10.3389/fpls.2015.01054.
Legave, J.M., Blanke, M., Christen, D., Giovannini, D., Mathieu, V., Oger, R., 2013. A comprehensive overview of the spatial and temporal variability of apple bud dormancy release and blooming phenology in Western Europe. Int. J. Biometeorol. 57, 317–331. https://doi.org/10.1007/s00484-012-0551-9.
Liang, X., Zhang, R., Gleason, M.L., Sun, G., 2022. Sustainable apple disease management in china: challenges and future directions for a transforming industry. Plant Dis. 106, 786–799. https://doi.org/10.1094/PDIS-06-21-1190-FE.
Liu, D.L., Zuo, H., 2012. Statistical downscaling of daily climate variables for climate change impact assessment over New South Wales, Australia. Clim. Change 115, 629–666. https://doi.org/10.1007/s10584-012-0464-y.
Lorite, I.J., Cabezas-Luque, J.M., Arquero, O., Gabaldón-Leal, C., Santos, C., Rodríguez, A., Ruiz-Ramos, M., Lovera, M., 2020. The role of phenology in the climate change impacts and adaptation strategies for tree crops: a case study on almond orchards in Southern Europe. Agric. . Meteorol. 294, 108142 https://doi.org/10.1016/j.agrformet.2020.108142.
Masaki, Y., 2019. Future risk of frost on apple trees in Japan. Clim. Change 159, 407–422. https://doi.org/10.1007/s10584-019-02610-7.
Meier, U., Graf, H., Hack, H., Hess, M., Kennel, W., Klose, R., Mappes, D., Seipp, D., Stauss, R.,Streif, J., 1994. Phenological growth stages of pome fruit (Malus domestica Borkh. and Pyrus communis L.), stone fruit (Prunus species), currants (Ribes species) and strawberry (Fragaria x ananassa Duch.). Nachrichtenbl. Deut. Pflanzenschutzd. 46, 141–153.
Melaas, E.K., Friedl, M.A., Richardson, A.D., 2016. Multiscale modeling of spring phenology across Deciduous Forests in the Eastern United States. Glob. Change Biol. 22, 792–805. https://doi.org/10.1111/gcb.13122.
Menzel, A., Sparks, T.H., Estrella, N., Roy, D.B., 2006. Altered geographic and temporal variability in phenology in response to climate change. Glob. Ecol. Biogeogr. 15, 498–504. https://doi.org/10.1111/j.1466-822X.2006.00247.x.
Migliavacca, M., Sonnentag, O., Keenan, T.F., Cescatti, A., O'Keefe, J., Richardson, A.D., 2012. On the uncertainty of phenological responses to climate change, and implications for a terrestrial biosphere model. Biogeosciences 9, 2063–2083. https://doi.org/10.5194/bg-9-2063-2012.
Pertille, R.H., Citadin, I., Oliveira, Ld.Sd, Broch, Jd.C., Kvitschal, M.V., Araujo, L., 2022. The influence of temperature on the phenology of apple trees grown in mild winter regions of Brazil, based on long-term records. Sci. Hortic. 305, 111354 https://doi.org/10.1016/j.scienta.2022.111354.
Pfleiderer, P., Menke, I., Schleussner, C.F., 2019. Increasing risks of apple tree frost damage under climate change. Clim. Change 157, 515–525. https://doi.org/10.1007/s10584-019-02570-y.
Polce, C., Garratt, M.P., Termansen, M., Ramirez-Villegas, J., Challinor, A.J., Lappage, M. G., Boatman, N.D., Crowe, A., Endalew, A.M., Potts, S.G., Somerwill, K.E., Biesmeijer, J.C., 2014. Climate-driven spatial mismatches between British orchards and their pollinators: increased risks of pollination deficits. Glob. Change Biol. 20, 2815–2828. https://doi.org/10.1111/gcb.12577.
Qiu, M., Liu, B., Liu, Y., Wang, K., Pang, J., Zhang, X., He, J., 2020. Simulation of first flowering date for apple and risk assessment of late frost in main producing areas of northern China (in Chinese with English abstract). Trans. CSAE 36, 154–163. https://doi.org/10.11975/j.issn.1002-6819.2020.21.01.
Rodríguez, A., Pérez-López, D., Centeno, A., Ruiz-Ramos, M., 2021. Viability of temperate fruit tree varieties in Spain under climate change according to chilling accumulation. Agric. Syst. 186, 102961 https://doi.org/10.1016/j.agsy.2020.102961.
Rosenzweig, C., Jones, J.W., Hatfield, J.L., Ruane, A.C., Boote, K.J., Thorburn, P., Antle, J.M., Nelson, G.C., Porter, C., Janssen, S., 2013. The agricultural model intercomparison and improvement project (AgMIP): protocols and pilot studies. Agric. . Meteorol. 170, 166–182.
Ru, X., Jiang, Y., Luo, Q., Wang, R., Feng, X., Wang, J., Wang, Z., Li, M., Qu, Z., Su, B., Feng, H., Zhang, D., Liu, D., Yu, Q., He, J., 2023. Evaluating late spring frost risks of apple in the Loess Plateau of China under future climate change with phenological modeling approach. Sci. Hortic. 308, 111604 https://doi.org/10.1016/j.scienta.2022.111604.
Ruane, A.C., Rosenzweig, C., Asseng, S., Boote, K.J., Elliott, J., Ewert, F., Jones, J.W., Martre, P., McDermid, S.P., Müller, C., 2017. An AgMIP framework for improved agricultural representation in integrated assessment models. Environ. Res. Lett. 12, 125003 https://doi.org/10.1088/1748-9326/aa8da6.
Storn, R., Price, K., 1997. Differential evolution–a simple and efficient heuristic for global optimization over continuous spaces. J. Glob. Optim. 11, 341–359. https://doi.org/10.1023/A:1008202821328.
Tang, W., Wang, W., Chen, D., Cui, N., Yang, H., Hu, X., 2021. Evaluation of the regional-scale optimal k rate based on sustainable apple yield and high-efficiency K use in Loess Plateau and Bohai Bay of China: a meta-analysis. Agronomy 11, 1368. https://doi.org/10.3390/agronomy11071368.
Tao, F., Rotter, R.P., Palosuo, T., Gregorio Hernandez Diaz-Ambrona, C., Minguez, M.I., Semenov, M.A., Kersebaum, K.C., Nendel, C., Specka, X., Hoffmann, H., Ewert, F., Dambreville, A., Martre, P., Rodriguez, L., Ruiz-Ramos, M., Gaiser, T., Hohn, J.G., Salo, T., Ferrise, R., Bindi, M., Cammarano, D., Schulman, A.H., 2018. Contribution of crop model structure, parameters and climate projections to uncertainty in climate change impact assessments. Glob. Change Biol. 24, 1291–1307. https://doi.org/10.1111/gcb.14019.
Taylor, S.D., Meiners, J.M., Riemer, K., Orr, M.C., White, E.P., 2018. Comparison of large-scale citizen science data and long-term study data for phenology modeling. Ecology 100, e02568. https://doi.org/10.1002/ecy.2568.

Wang, M., Liu, B., Liu, Y., Yang, X., Han, S., Qiu, M., Li, Q., 2020. Assessment on the freezing Injury risk during apple flowering in Liquan and Xunyi (in Chinese with English abstract). Chin. J. Agrometeorol. 41, 381–392. https://doi.org/10.3969/j.issn.1000-6362.2020.06.005.

Wang, R., Ru, X., Jiang, T., Wang, J., Wang, Z., Su, B., Zhang, D., Yu, Q., Feng, H., He, J., 2021. Based on the phenological model to study the possible changes of apple flowering dates under future climate scenarios in Shaanxi Province (in Chinese with English abstract). Chin. J. Agrometeorol. 42, 729–745. https://doi.org/10.3969/j.issn.1000-6362.2021.09.002.

Wilcock, C., Neiland, R., 2002. Pollination failure in plants: why it happens and when it matters. Trends Plant Sci. 7, 270–277. https://doi.org/10.1016/S1360-1385(02)02258-6.

Wypych, A., Sulikowska, A., Ustrnul, Z., Czekierda, D., 2017. Variability of growing degree days in Poland in response to ongoing climate changes in Europe. Int. J. Biometeorol. 61, 49–59. https://doi.org/10.1007/s00484-016-1190-3.

Wyver, C., Potts, S.G., Edwards, R., Edwards, M., Senapathi, D., 2023. Climate driven shifts in the synchrony of apple (Malus x domestica Borkh.) flowering and pollinating bee flight phenology. Agric. . Meteorol. 329, 109281 https://doi.org/10.1016/j.agrformet.2022.109281.

Xiao, L., Liu, L., Asseng, S., Xia, Y., Tang, L., Liu, B., Cao, W., Zhu, Y., 2018. Estimating spring frost and its impact on yield across winter wheat in China. Agric. . Meteorol. 260–261, 154–164. https://doi.org/10.1016/j.agrformet.2018.06.006.

Yan, B., Pascual, J., Bouchard, M., D'Orangeville, L., Perie, C., Girardin, M.P., 2021. Multi-model projections of tree species performance in Quebec, Canada under future climate change. Glob. Change Biol. 28, 1884–1902. https://doi.org/10.1111/gcb.16014.

Yoder, K., Yuan, R., Combs, L., Byers, R., McFerson, J., Schmidt, T., 2009. Effects of temperature and the combination of liquid lime sulfur and fish oil on pollen germination, pollen tube growth, and fruit set in apples. Hortscience 44, 1277–1283. https://doi.org/10.21273/HORTSCI.44.5.1277.